



RV College of Engineering®

Autonomous institution affiliated
to Visvesvaraya Technological
University, Belagavi | Approved by AICTE, New Delhi

Go, change the world

Battery Management System For Implantable Pacemakers

A Minor Project Report

18EC64

Submitted by,

Neha Dao

1RV18EC096

R Vibha Narayan

1RV18EC121

Raghavendra P R

1RV18EC123

Rahul Pinny

1RV18EC125

Under the guidance of

Dr. Shilpa D R

Associate Professor

Dept. of ECE

RV College of Engineering

In partial fulfillment of the requirements for the degree of
Bachelor of Engineering in
Electronics and Communication Engineering
2020-2021

RV College of Engineering[®], Bengaluru

(Autonomous institution affiliated to VTU, Belagavi)

Department of Electronics and Communication Engineering



CERTIFICATE

Certified that the minor project (18EC64) work titled ***Battery Management System For Implantable Pacemakers*** is carried out by **Neha Dao (1RV18EC096)**, **R Vibha Narayan (1RV18EC121)**, **Raghavendra P R (1RV18EC123)** and **Rahul Pinny (1RV18EC125)** who are bonafide students of RV College of Engineering, Bengaluru, in partial fulfillment of the requirements for the degree of **Bachelor of Engineering in Electronics and Communication Engineering** of the Visvesvaraya Technological University, Belagavi during the year 2020-2021. It is certified that all corrections/suggestions indicated for the Internal Assessment have been incorporated in the minor project report deposited in the departmental library. The minor project report has been approved as it satisfies the academic requirements in respect of minor project work prescribed by the institution for the said degree.

Signature of Guide Signature of Head of the Department Signature of Principal

Dr. Shilpa D R

Dr. K S Geetha

Dr. K N Subramanya

External Viva

Name of Examiners

Signature with Date

1.

2.

DECLARATION

We, Neha Dao, R Vibha Narayan, Raghavendra P R and Rahul Pinny students of sixth semester B.E., Department of Electronics and Communication Engineering, RV College of Engineering, Bengaluru, hereby declare that the minor project titled '**Battery Management System For Implantable Pacemakers**' has been carried out by us and submitted in partial fulfilment for the award of degree of **Bachelor of Engineering in Electronics and Communication Engineering** during the year 2020-2021.

Further we declare that the content of the dissertation has not been submitted previously by anybody for the award of any degree or diploma to any other university.

We also declare that any Intellectual Property Rights generated out of this project carried out at RVCE will be the property of RV College of Engineering, Bengaluru and we will be one of the authors of the same.

Place: Bengaluru

Date:

Name

Signature

1. Neha Dao(1RV18EC096)
2. R Vibha Narayan(1RV18EC121)
3. Raghavendra P R(1RV18EC123)
4. Rahul Pinny(1RV18EC125)

ACKNOWLEDGEMENT

We are indebted to our guide, **Dr. Shilpa D R**, Associate Professor, RV College of Engineering . for the wholehearted support, suggestions and invaluable advice throughout our project work and also helped in the preparation of this thesis.

We also express our gratitude to our panel members **Mrs. Deepika P**, Assistant Professor and **Dr. Shilpa D R**, Associate Professor, Department of Electronics and Communication Engineering for their valuable comments and suggestions during the phase evaluations.

Our sincere thanks to the project coordinators **Prof. Subrahmanyam K N**, **Dr Nithin M** and **Dr Veena Devi** for their timely instructions and support in coordinating the project.

Our gratitude to **Prof. Narashimaraja P** for the organized latex template which made report writing easy and interesting.

Our sincere thanks to **Dr. K S Geetha**, Professor and Head, Department of Electronics and Communication Engineering, RVCE for the support and encouragement.

We express sincere gratitude to our beloved Principal, **Dr. K N Subramanya** for the appreciation towards this project work.

We thank all the teaching staff and technical staff of Electronics and Communication Engineering department, RVCE for their help.

Lastly, we take this opportunity to thank our family members and friends who provided all the backup support throughout the project work.

ABSTRACT

Implantable devices are used in various biomedical applications and are powered using rechargeable or non rechargeable batteries. Life-saving implantable medical devices like pacemakers face a major drawback of battery charge depletion run out and the patients have to undergo frequent surgeries to have them replaced. With the advent of modern technology, many solutions can be provided for reducing the frequency of such surgeries. One of the solutions is to power these devices by converting the vibrational energy from the body to electrical energy which can then be used to charge the battery thereby increasing its life span.

The proposed design consists of many individual circuits of which the charge pump and the operational transconductance amplifier are the most important. A charge pump is a voltage multiplier circuit designed using MOSFETs and capacitors. The charge pump used in the integrated circuit is called a cross coupled charge pump which is derived from the popular Dickson charge pump. An operational transconductance amplifier (OTA) is a voltage controlled constant current source. A telescopic OTA is used in the proposed design. Our proposed design of the battery charger circuit takes the low input voltage from an energy harvesting element which is then amplified using the charge pump circuit. This amplified voltage is given as an input to the OTA to get a constant current output which can be used to charge the lithium ion battery of the pacemaker.

All the design and simulations have been carried out in Cadence Virtuoso software considering the ideal case, where a constant input voltage of 1.2 V is considered. All the MOSFETs are of 90 nm technology which are available in the gpdk090 library in the software. The cross coupled charge pump gives an output voltage of 5.83 V under no load condition and 4.82 V with load. The OTA gives a constant output current of 12.22 uA. The complete integrated system shows the total dc power to be 171.76 uW. The modelling and simulation of a lithium ion battery used to power the pacemaker is carried out in LTSpice software. A battery of capacity 5 mAh has been modelled in the software which takes about 10 days to deplete when a constant load of 20.8 uA is driven with the battery.

CONTENTS

Abstract	i
List of Figures	iv
List of Tables	vi
1 INTRODUCTION TO BATTERY MANAGEMENT SYSTEM IN IMPLANTABLE DEVICES	1
1.1 Introduction	2
1.2 Motivation	2
1.3 Problem statement	3
1.4 Objectives	3
1.5 Literature Review	3
1.6 Brief Methodology of the project	4
1.7 Assumptions made / Constraints of the project	5
1.8 Organization of the report	6
2 FUNDAMENTALS OF CHARGE PUMPS AND BATTERY	7
2.1 Charge Pump	8
2.1.1 Cockcroft Walton Voltage Multiplier	9
2.2 Battery	11
3 TOPOLOGIES OF CHARGE PUMPS	13
3.1 Cockcroft Walton Voltage Multiplier	14
3.2 Dickson Charge Pump	15
3.3 Cross Coupled Charge Pump	20
3.4 Cross Coupled Charge Pump with Bulk Biasing	25
3.5 Comparison	27
4 ADDITIONAL CIRCUITS: OPERATIONAL TRANSCONDUCTANCE AMPLIFIER, OSCILLATOR AND BATTERY CIRCUIT	29
4.1 Operational Trans-conductance Amplifier	30

4.2	Oscillator	32
4.3	Battery Circuit	33
5	Results & Discussion	41
5.1	Integrated circuit	42
5.2	Simulation of the integrated circuit	43
6	Conclusion and Future Scope	45
6.1	Conclusion	46
6.2	Future Scope	46
6.3	Learning Outcomes of the Project	47



LIST OF FIGURES

1.1	Methodology	5
2.1	A Generalised Charge Pump	9
2.2	Single stage Cockcroft Walton VM	9
2.3	2 stage Cockcroft Walton voltage multiplier	10
3.1	Cockcroft Walton 2 stage schematic	14
3.2	Transient Analysis of 2 stage Cockcroft Walton VM	14
3.3	Dickson charge pump with diodes	15
3.4	Dickson charge pump with MOSFETs	15
3.5	Voltage waveforms in an N-stage charge multiplier showing voltage relationship between nodes of the diode chain	16
3.6	Equivalent circuit of an N-stage multiplier	16
3.7	A one stage Dickson Charge Pump	18
3.8	A 4-stage Dickson Charge Pump	19
3.9	Transient analysis output of 4-stage Dickson charge pump	19
3.10	DC analysis and power plot outputs of 4-stage Dickson charge pump	19
3.11	Single stage cross coupled charge pump with a clock source	20
3.12	Timing diagram of cross coupled charge pump	20
3.13	Circuit explaining the lost charge parasitics in phase 1	21
3.14	Half circuit modelled during phase 1 when load is connected	22
3.15	Four stage schematic of cross coupled charge pump in transistor level	23
3.17	Transient response with current plot along with output voltage	23
3.16	Block level schematic of four stage cross coupled charge pump	24
3.18	Transient analysis of output voltage after four stages	24
3.19	DC analysis of four stage cross coupled charge pump	24
3.20	Generalised circuit for body biasing technique	25
3.21	Single Stage Cross coupled CP with Bulk Switching	26
3.22	Schematic of single stage	26
3.23	2 stage Cross Coupled CP with Bulk Biasing block diagram	26
3.24	Transient Analysis with Current plot and output voltage	27

3.25 DC analysis of with output voltage	27
4.1 Ideal OTA model	30
4.2 Schematic of the OTA	31
4.3 Transient response of the OTA	32
4.4 Ring oscillator with buffers	32
4.5 Output of the oscillator	33
4.6 State of Charge Model	34
4.7 The IR Model of Rechargeable Li Ion Battery	34
4.8 The IR Model of Rechargeable Li Ion Battery	35
4.9 Li Ion battery's Characteristics waveform for battery voltage and current during charging and discharging	36
4.10 Discharge Curve of TTC Model Li Ion Battery	38
4.11 Discharge of Li Ion Battery Model for Different load currents	38
4.12 Output of Discharge of Li Ion Battery for Different load currents	38
4.13 Charging and discharging of Li Ion Battery Model	39
4.14 Input Current Pulse	39
4.15 Battery voltage level with time	40
4.16 State of Charge of the Battery	40
5.1 Block diagram representation of the integrated circuit	42
5.2 Schematic diagram of the integration of cross coupled charge pump with OTA	43
5.3 Transient response of the integrated circuit	43
5.4 DC response of the integrated circuit with power plot	43

LIST OF TABLES

3.1 Comparison of charge pump topologies	27
--	----



A circular watermark logo for 'Rashtreeya Sikshana Samithi Trust'. It features a stylized 'RV' monogram in the center, with 'Rashtreeya Sikshana Samithi Trust' written in a semi-circle around it. A registered trademark symbol (®) is located at the top right of the circle.

®

Chapter 1

INTRODUCTION TO BATTERY MANAGEMENT SYSTEM IN IMPLANTABLE DEVICES

CHAPTER 1

INTRODUCTION TO BATTERY MANAGEMENT SYSTEM IN IMPLANTABLE DEVICES

1.1 Introduction

Wearable electronics and implants have their applications in various domains such as aerospace, defence, medicine and so on. Wearable electronics were invented as far back as the 1960s where Edward Thorp and Claude Shannon had developed a basic calculator that could fit inside a shoe. Implantable devices, usually sensors, are widely used in various biomedical applications. An important factor about such a device is to function without a plugged in power source. Usually batteries are used to power such devices - rechargeable or non rechargeable [1]. Rechargeable batteries need an external energy source whereas non rechargeable batteries have to be replaced periodically and replacing them exposes an individual to unnecessary dangers as biomedical implants operate in environments which are not easy to access. Hence the idea of self powering such devices came to light using small energy sources which harvest energy using the physical processes occurring in the organs. Harnessing energy by such means requires sophisticated circuitry which has to produce sufficient power and also fit in a limited space. Various energy harvesting and charging techniques have been introduced by many researchers over a period of time such as using piezoelectric devices to harvest charges due to vibrations and utilising it for charging the battery, using electrostatic devices and so on [2]. A few designs of the battery charging circuit carry out wireless charging of the battery in the device. The proposed design focuses on charging the battery appropriately so that the implant functions at its normal capacity.

1.2 Motivation

Almost all of the wearable electronic devices face the problem of poor battery life. This is a major problem to the users as the device might shut down unexpectedly. As these devices are responsible for vital biological functions, their non functioning can pose a huge threat to a patient's life. These devices undergo continuous motion which can be used as a source of energy to produce electrical energy using piezoelectric devices, motion sensing devices and so on. This produced electrical energy can be used to replenish

the on-chip power supply thereby preventing low battery levels and ensuring that the biological functions are carried out perfectly.

1.3 Problem statement

Designing an optimised charge transfer circuit to recharge the battery of the implant using MOSFETs, resistors, capacitors etc. to meet the above mentioned requirement.

1.4 Objectives

The objectives of the project are:

1. To design a circuit to transfer electric charge from the harvesting element to the battery at regular intervals.
2. Explore various topologies to increase the efficiency of the conversion and charging processes, to reduce overhead energy losses, to reduce the overall size of the circuit and to make the device cost efficient.

1.5 Literature Review

Literature review forms an integral part of any project. After surveying various publications, including journals and papers, we decided to design the final integrated circuit using a charge pump as the voltage amplification block.

The mechanical energy in vibrations, which are naturally abundant in many practical applications, have been scavenged and channeled to a rechargeable battery. The proposed system extends the operational life of the system indefinitely without any external replacement of the battery or manual recharging.[2]

In paper [3] the clockwork mechanism of an automatic wristwatch has been utilized for energy harvesting by optimising its oscillation weight using mathematical models. The average impulse energy is constant because parameters such as spring stiffness, transmission gear ratio or load resistance are considered to be constants and secondary batteries and capacitors are used as buffers to store the generated charge. A strong relation between the harvested amount of energy and the position and orientation of the device in the heart is also revealed.

The Magnetic Resonance coupling - a wireless power transfer system for achieving high efficiency [4]. It proposes a battery charging unit using rectifiers, filters, a voltage stabilization circuit, etc. It also comprises various safety methods such as temperature

monitoring and EMC for human tissues. Furthermore, it also shows that prolonged exposure to such devices may be harmful to human beings due to electromagnetic interference.

A battery charging circuit which consists of a voltage reference circuit, operational transconductance amplifier, current gain stage, trickle charge and end of charge detector circuits. The design works on the principle of constant current constant voltage method of charging. The circuit is highly efficient and occupies very less area. [5]

The charger circuit given in paper [6] uses the tanh output current profile of an operational transconductance amplifier to switch smoothly between constant current and constant voltage charging regimes without the need for additional area- and power-consuming control circuitry. A low power detector circuit is also designed to prevent damage to the battery due to deep discharge.

An effective wireless power transfer (WPT) system using transmitter and receiver coils and a cardiac pacemaker whose battery is charged wirelessly at a frequency of 160 KHz is presented in [7].

A battery charge meter, to monitor the battery life is presented in [8]. The output voltage of the implemented circuit may steeply drop during the end of life of the battery. Also, a switched capacitor voltage controlled oscillator is implemented. Since the IC consumes less power, it is expected to increase the lifetime of the device used in biomedical applications.

Paper [9] has a two battery based power management system. It consists of a supply detector and a charge detector for facilitating the power management. A charger circuit is employed to provide a constant current to charge the batteries.

An integration strategy for directly powering a modern fully-functional cardiac pacemaker by harvesting the natural energy of a heartbeat is given in paper [10]. The implantable piezoelectric energy generator has a capability of generating the maximal output voltage of about 20 V and a short circuit current of about 8 A in series mode and about 12 V and 15 A respectively in parallel mode. A commercial cardiac pacemaker is directly driven by this implantable piezoelectric energy generator.

A brief study of different methods of energy harvesting techniques for implantable devices along with self powering the devices have been explained in paper [11].

1.6 Brief Methodology of the project

The project meets the objectives by following the methodology as in Figure 1.1:

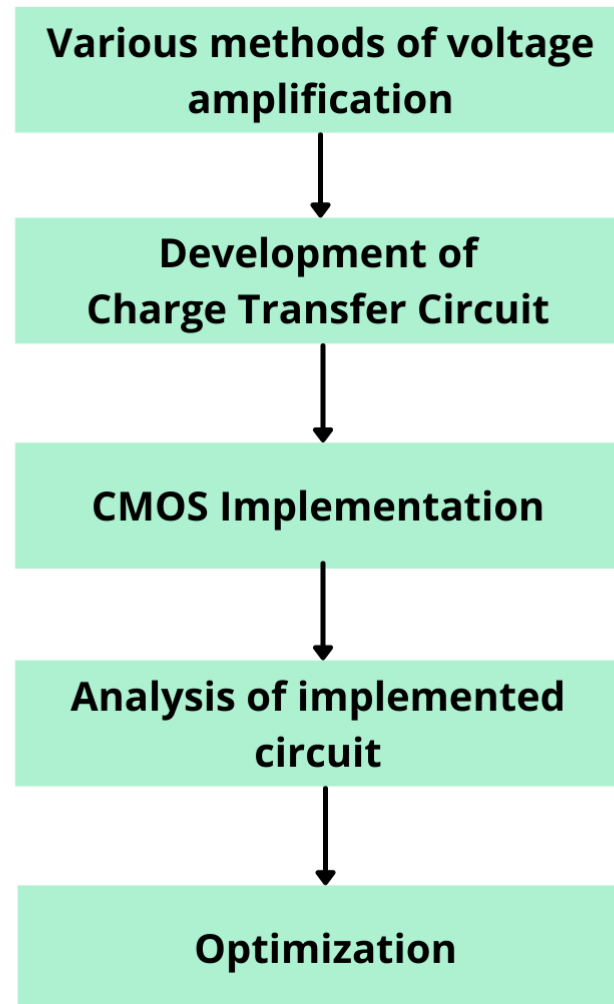


Figure 1.1: Methodology

- To conduct an extensive study about various methods of voltage amplification.
- To design the charge transfer circuit by combining the necessary blocks.
- To carry out the CMOS implementation of the circuit in Cadence Virtuoso.
- To simulate the integrated circuit in transient and DC modes to determine the variations in various parameters.
- To optimise the integrated circuit to meet our requirements.

1.7 Assumptions made / Constraints of the project

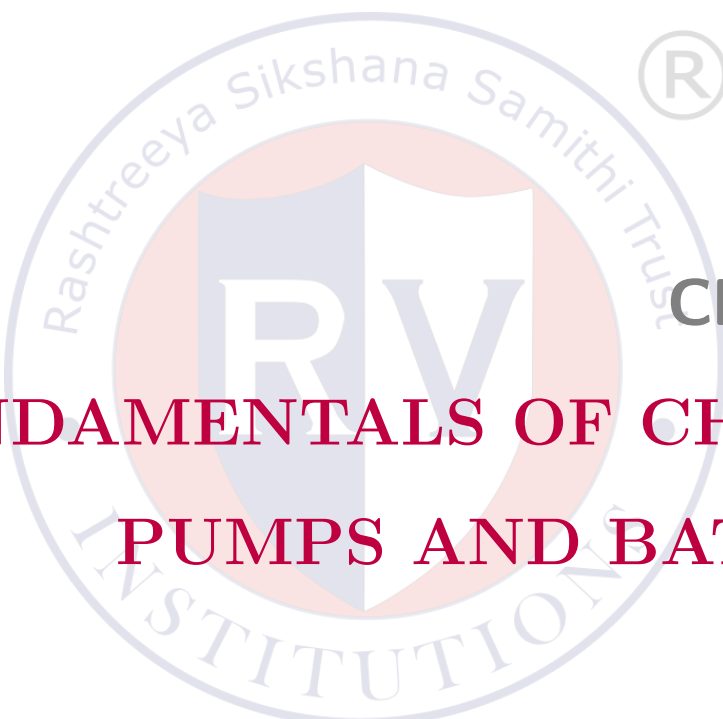
The design can be modified to work with different supply voltages. Ideal or favourable conditions have been assumed in the development of the circuit. A voltage source of 1.2V

is used as the supply voltage, for simulation and demonstration purposes, which may not be true in real life situations. Simulation of the integrated circuit has been carried out using Cadence Virtuoso and that of the battery is carried out using LTSpice.

1.8 Organization of the report

This report is organized as follows:

- Chapter 2 discusses the fundamentals of charge pumps and batteries.
- Chapter 3 discusses about the topologies of charge pumps, their design and implementation.
- Chapter 4 discusses about the additional circuits that have been implemented in order to arrive at an integrated charging circuit. The additional circuits implemented are operational transconductance amplifier (OTA), oscillator along with the modelling and simulation of the battery used in the pacemaker devices.
- Chapter 5 gives insights about the integrated circuit .
- Chapter 6 deals with the final outline of the results and the methods to possibly improve the current design .



The logo watermark of RV College of Engineering is a circular emblem. It features a stylized 'RV' monogram in the center, with 'Rashtriya Sikshana Samithi Trust' written around it in a circular path. Below the monogram, the word 'INSTITUTION' is written vertically.

Chapter 2

**FUNDAMENTALS OF CHARGE
PUMPS AND BATTERY**

CHAPTER 2

FUNDAMENTALS OF CHARGE PUMPS AND BATTERY

In implantable devices like the pacemaker, a continuous and uninterrupted supply voltage is required for its proper functioning thereby protecting the patient. The battery needs to be recharged periodically from an external source which is a complicated process or use the available energy source present nearby like the vibration energy, solar energy, thermal energy etc. to replenish the charge. The voltage obtained from such a source is very small, in the range of millivolts or even lesser. Therefore there is a requirement of a DC - DC step up converter which generates higher voltage using the available low voltage. This chapter also lists the characteristics of batteries.

2.1 Charge Pump

A very common challenge in circuits is the need to convert an available DC source to a lower or higher voltage. For the high-to-low conversion, one option is to use a low dropout regulator (LDO regulator). The difficulty arises in the case of low to high conversion. While in AC signals it is common to use a transformer for the conversion, the same principle can't be applied for DC signals. A rectifier and filter can be used in addition to the transformer to get a regulated output, however, this increases the complexity and the size of the circuit. Charge pumps have become an excellent alternative to this and are also considered IC friendly [12]. A charge pump is a kind of DC-to-DC converter that uses capacitors for energetic charge storage to raise or lower voltage. Charge-pump circuits are capable of high efficiencies, sometimes as high as 90–95 percent , while being electrically simple circuits. It uses capacitors as the energy-storage element. In the basic execution of this power-conversion technique, current (charge) is alternately switched and directed between two capacitors arranged so the circuit output is twice the input, and thus functioning as a voltage-doubling boost converter [13]. For these reasons, the charge-pump converter is also known as a switched-capacitor design as shown in Figure 2.1.

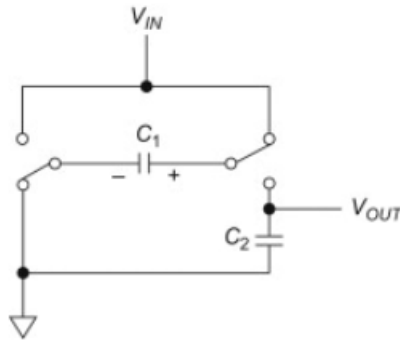


Figure 2.1: A Generalised Charge Pump

2.1.1 Cockcroft Walton Voltage Multiplier

Cockcroft-Walton (CW) is a voltage multiplier (VM) circuit with an alternating current (AC) input to generate a direct current (DC) output. The CW circuit may consist of several stages depending on the application. Each stage, there are two diodes and capacitors to shift the AC input to DC output as shown in the Figure 2.2. The maximum output of CW is the multiplication of two and number of stages, then the multiplied result times the peak voltage of AC input to obtain the DC voltage [14].

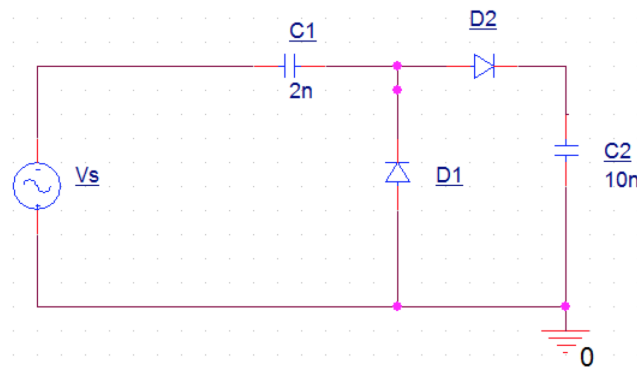


Figure 2.2: Single stage Cockcroft Walton VM

1. Working: When source voltage V_s on its negative peak, diode D_1 is forward biased and capacitor C_1 gets charged to the peak source voltage V_m . Using ideal diodes leads to no voltage differential across capacitor C_2 , thereby no stored charge. On the positive half cycle, the peak voltage from the source is now in series with the voltage differential across capacitor C_1 , so they add together. Diode D_1 is now reverse biased with a voltage difference of twice the magnitude of the peak source

voltage. Diode D_2 and capacitor C_2 work to reduce the ripple voltage of the output waveform. Ideally, this creates a voltage differential across capacitor C_2 which is equal to twice the magnitude of the peak source voltage. The current theory assumes ideal diodes and that the capacitors charge near-instantaneously. In reality, it will take several cycles for the voltage across C_2 to reach its peak at $2V_m$ [15]. The Figure 2.3 depicts a basic of two stages CW circuit. It involves two capacitor

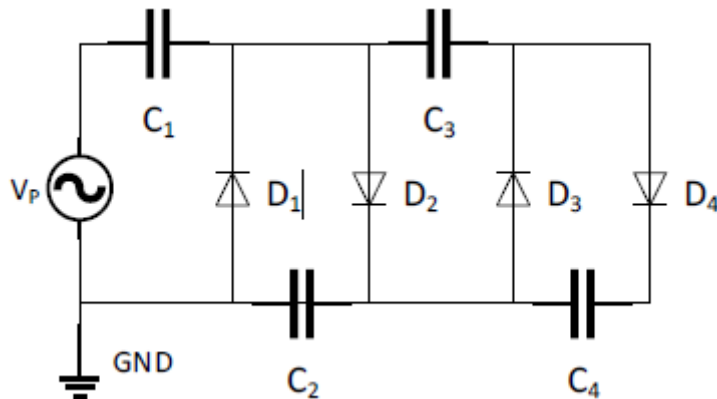


Figure 2.3: 2 stage Cockcroft Walton voltage multiplier

columns, specifically oscillating and smoothening columns. The oscillating column capacitors (C_1 and C_3) are charged by facing up diodes (D_1 and D_3) in the negative cycle. Then, smoothening column capacitors (C_2 and C_4) are charged in the next half-cycle by facing down diodes (D_2 and D_4). In no-load condition, smoothening column capacitors were charged until two times peak voltage of input $2V_p$ [14].

$$\text{Total peak voltage at output} = 2nV_p$$

Where n = no. stages , here , n=2

In CW voltage multiplier, the output obtained is pulsated DC and the ripple voltage increases with the no. of stages. This shows a tradeoff between the need of higher voltage and added ripple to the output signal as in equation (2.1) and equation (2.2).

$$\Delta V_O = \frac{I}{fC} \left(\frac{2}{3}n^3 + \frac{1}{2}n^2 - \frac{n}{6} \right) \quad (2.1)$$

$$\Delta V_O = \frac{V_P}{RfC} \left(\frac{2}{3}n^3 + \frac{1}{2}n^2 - \frac{n}{6} \right) \quad (2.2)$$

This is the basis for all the other charge pump topologies implemented using MOS-FETs.

2.2 Battery

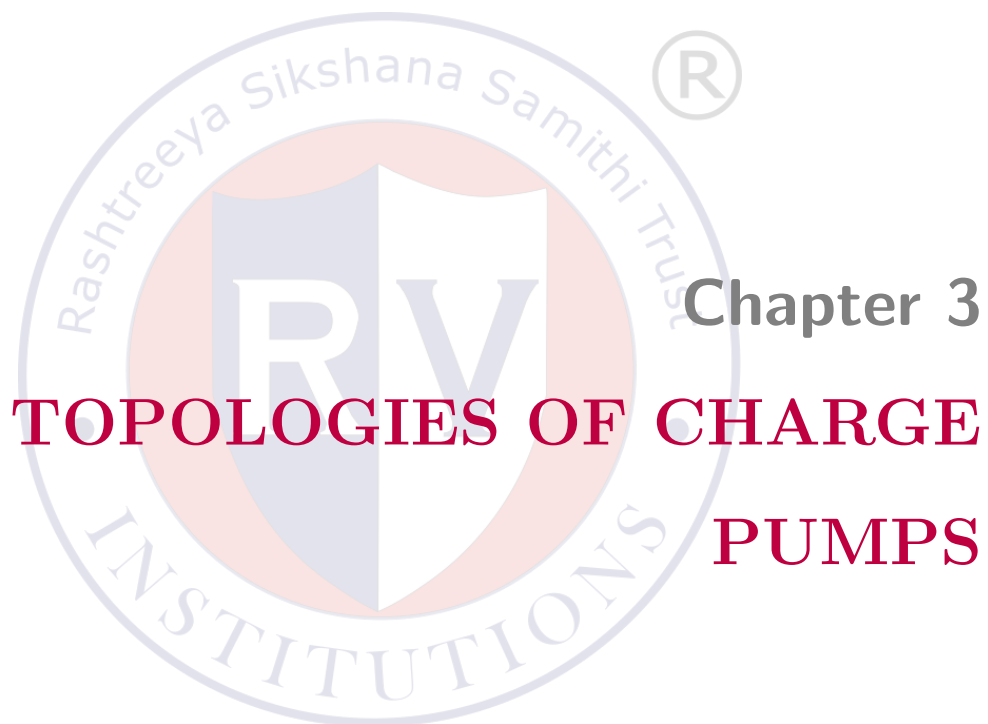
Batteries designed for the use of biomedical devices have helped to facilitate the successful delivery of devices and their treatment of human diseases. These biomedical devices are permanently placed in the human body to monitor and provide the required treatment on a timely basis or as required. While the operating requirements for batteries used to power these devices vary in device type and treatment, with some common characteristics demanded by all applications.

The important characteristics of battery that are used to power the implantable medical devices are [1]

- It must work for a long period of time thereby reducing the frequency of surgical operation.
- It must be safe while installing and use and also provide tolerance to mechanical and electrical abuse.
- Its performance must be predictable which helps in studying the state of discharge of the battery.
- It must be highly reliable which means variations in performance parameters must be low.
- It must have volumetric high energy density to provide devices of smaller size, low weight and comfort for the patients holding it.
- It must be of low self-discharge which means the battery capacity must not degrade drastically on usage.
- It must be able to indicate its end of life during both loaded and unloaded voltage conditions.

Batteries are classified into two types, the primary batteries which are used once and discarded while the other being secondary batteries or rechargeable batteries which are used continuously by periodical recharging with help of an additional charging circuitry and external source thereby increasing the longevity of the battery and its average power. A successful recharging of the battery used in the pacemaker by inductive coupling was demonstrated in the late 1960s. The most commonly used battery in pacemaker devices, which requires current in microampere range for its functioning, is the rechargeable Li Ion battery due to its high energy density, high voltage and low self-discharge [9].





CHAPTER 3

TOPOLOGIES OF CHARGE PUMPS

A detailed study on DC-DC converters has been done in the literature survey, and looking at the requirements for the application, charge pump is chosen. Various topologies of charge pumps are studied and simulated on the Cadence Virtuoso tool. Four different topologies of charge pumps , namely Cockcroft walton, Dickson charge pump, Cross coupled charge pump and Cross coupled charge pump with body biasing, are presented in the current chapter.

3.1 Cockcroft Walton Voltage Multiplier

1. Simulation: In the implementation of the previously discussed topology, a NMOS

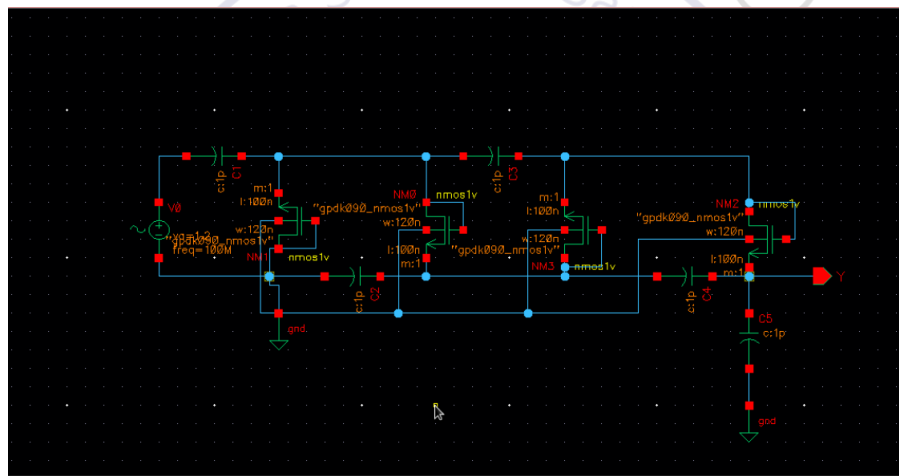


Figure 3.1: Cockcroft Walton 2 stage schematic

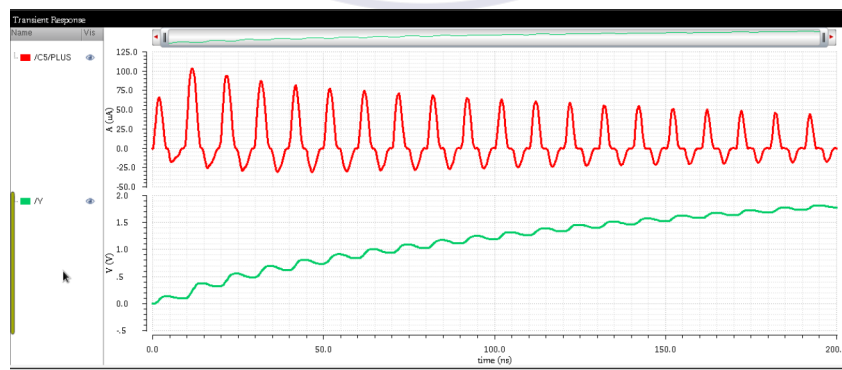


Figure 3.2: Transient Analysis of 2 stage Cockcroft Walton VM

diode connected load is used instead of a conventional diode to make it a CMOS implementation and for comparison as in Figure 3.1 and the transient analysis is

been evaluated as Figure 3.2 where there is increase in voltage but with much ripples.

3.2 Dickson Charge Pump

It is hard to generate output voltages higher than double of the power supply voltage with any number of stages using Cockcroft– Walton voltage multiplier circuit. When the number of stages is increased beyond three or four stages in the Cockcroft–Walton voltage multiplier, the output voltage starts falling due to the threshold voltage drop in diodes. In 1976, John F. Dickson modified the Cockcroft–Walton voltage multiplier circuit and developed a new voltage multiplier circuit. Dickson attached the pumping capacitors in parallel, which resulted in an inferior output impedance and superior voltage gain as the number of stages was increased in order to resolve the problem seen in the Cockcroft - Walton voltage multiplier circuit [13]. A four stage Dickson charge pump is constructed using diodes and capacitors as shown in Figure 3.3. Similarly, the diodes could be replaced with MOSFETs as shown in Figure 3.4.

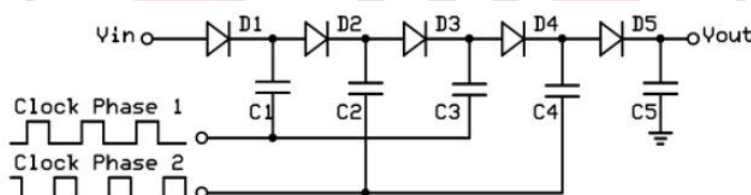


Figure 3.3: Dickson charge pump with diodes

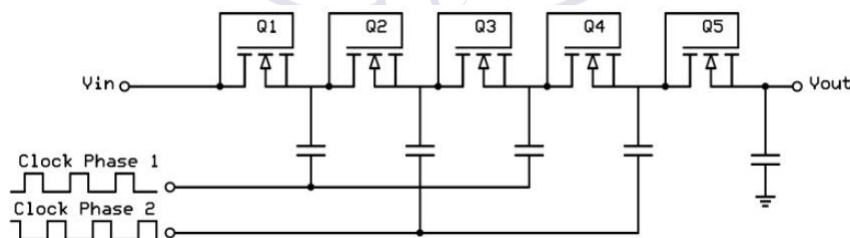


Figure 3.4: Dickson charge pump with MOSFETs

where V_{in} = Input voltage, V_{out} = Output voltage

1. Working and Modelling: The two clock signals ϕ and ϕ' are in antiphase with amplitude V_ϕ , and are capacitively coupled to alternate nodes along the chain. The

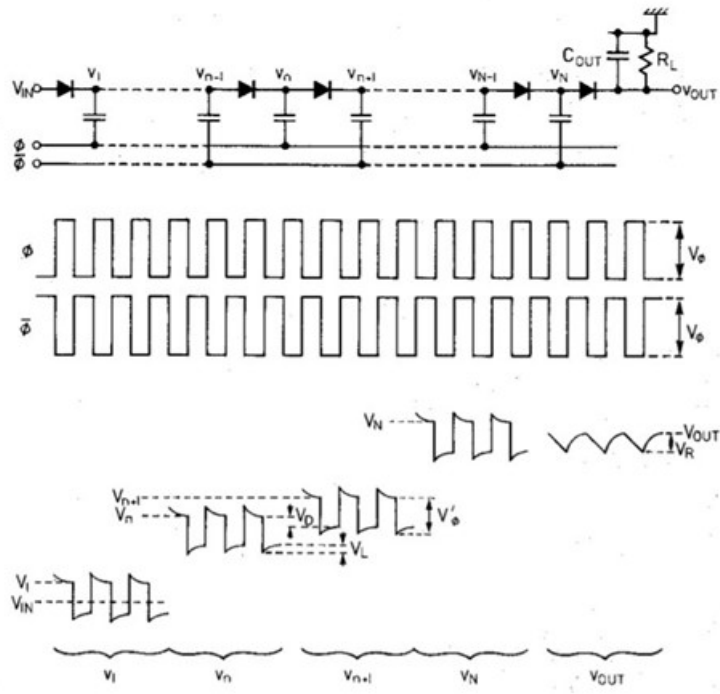
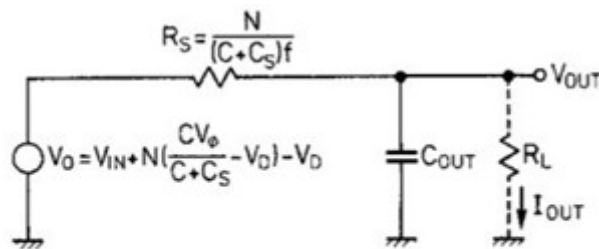


Figure 3.5: Voltage waveforms in an N -stage charge multiplier showing voltage relationship between nodes of the diode chain

multiplier operates by pumping packets of charge along the diode chain as the coupling capacitors are successively charged and discharged during every half clock cycle. The voltages in the diode chain are not reset after each pumping cycle so that the average node potentials increase in progression from the input to the output of the chain of diodes. Here, the coupling capacitor is connected to the input clock [12]. As seen in Figure 3.5, the difference in voltages of the n^{th} and $n + 1^{th}$ nodes at the end of each pumping cycle is given by equation (3.1)

$$V_{n+1} - V_n = V'_\phi - V_D - V_L \quad (3.1)$$



$$V_{OUT} = V_0 - I_{OUT} R_S$$

Figure 3.6: Equivalent circuit of an N -stage multiplier

where V'_ϕ is the voltage swing at every node due to capacitive coupling from the clock, V_D is the forward bias voltage or the forward voltage drop of the diode, and V_L is the voltage by which the capacitors are charged and discharged when the circuit is producing an output current, I_{OUT} . Capacitance division, for a clock coupling capacitance, C, and stray capacitance C_S , at each node, gives V'_ϕ as in equation (3.2).

$$V'_\phi = \left(\frac{C}{C + C_S} \right) \cdot V_\phi \quad (3.2)$$

The total charge pumped by each diode per clock cycle is $(C + C_S) V_L$ and the current supplied by the multiplier at a clock frequency, f, is given by

$$I_{OUT} = f (C + C_S) V_L \quad (3.3)$$

Equation (3.4) is obtained by substituting V'_ϕ and V_L in equation (3.3),

$$V_{n+1} - V_n = \left(\frac{C}{C + C_S} \right) \cdot V_\phi - V_D - \frac{I_{OUT}}{(C + C_S) f} \quad (3.4)$$

Equation (3.5) provides for N stages,

$$V_N - V_{IN} = N \left[\left(\frac{C}{C + C_S} \right) \cdot V_\phi - V_D - \frac{I_{OUT}}{(C + C_S) f} \right] \quad (3.5)$$

where V_{IN} is the input voltage. An additional isolating diode is required in a practical multiplier at the output to prevent clock breakthrough so that the peak output voltage, V_{OUT} , is given by equation (3.6).

$$V_{OUT} - V_{IN} = N \left[\left(\frac{C}{C + C_S} \right) \cdot V_\phi - V_D - \frac{I_{OUT}}{(C + C_S) f} \right] - V_D \quad (3.6)$$

Rearranging,

$$V_{OUT} = V_{IN} + N \left[\left(\frac{C}{C + C_S} \right) \cdot V_\phi - V_D \right] - V_D - \frac{NI_{OUT}}{(C + C_S) f} \quad (3.7)$$

From equation (3.7), it can be seen that voltage multiplication occurs, provided

that equation (3.8) is satisfied.

$$\left(\frac{C}{C + C_S} \right) \cdot V_\phi - V_D - \frac{I_{\text{OUT}}}{(C + C_S) f} > 0 \quad (3.8)$$

It is important to note that this expression is independent of the number of stages, N , so theoretically there is no limit in this multiplier. The current drive capability of the multiplier is also independent of the number of multiplier stages provided Equation (3.10) is satisfied. From Equation (3.9),

$$V_{\text{OUT}} = V_O - I_{\text{OUT}} R_S \quad (3.9)$$

where

$$V_O = V_{\text{IN}} - V_D + N \left[\left(\frac{C}{C + C_S} \right) \cdot V_\phi - V_D \right] \quad (3.10)$$

and

$$R_S = \frac{N}{(C + C_S) f} \quad (3.11)$$

V_O and R_S are the open-circuit output voltage and output series resistance of the multiplier so that equation (3.11) leads to a simple equivalent circuit of the multiplier output, as shown in Figure 3.6. In the case where MOS transistors are used instead of diodes, the diode forward voltage, V_D , is replaced by the MOS threshold voltage, V_T , in equation (3.9), providing equation (3.12)

$$V_{\text{OUT}} = V_{\text{IN}} - V_T + N \left[\left(\frac{C}{C + C_S} \right) \cdot V_\phi - V_T \right] - \frac{N I_{\text{OUT}}}{(C + C_S) f} \quad (3.12)$$

2. Simulation: A single stage Dickson charge pump can be designed using an n

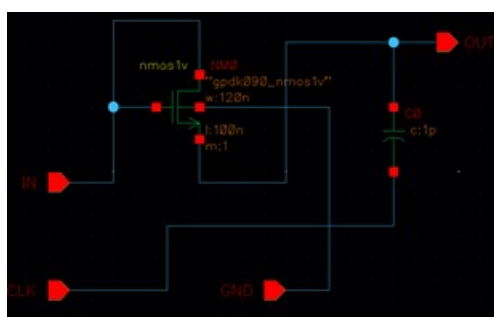


Figure 3.7: A one stage Dickson Charge Pump

type MOSFET and a capacitor by connecting it as shown in Figure 3.7. Here, for

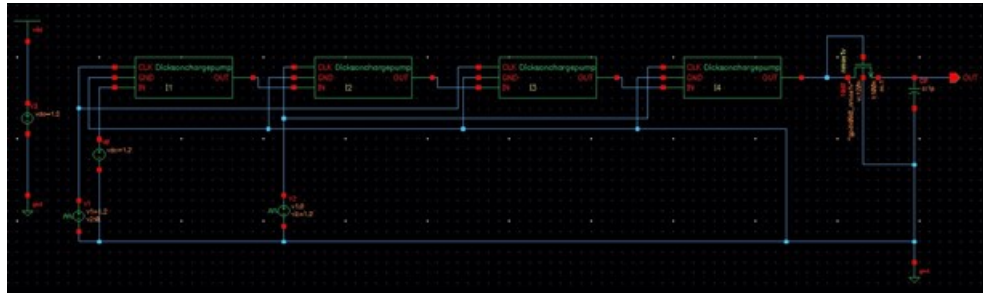


Figure 3.8: A 4-stage Dickson Charge Pump

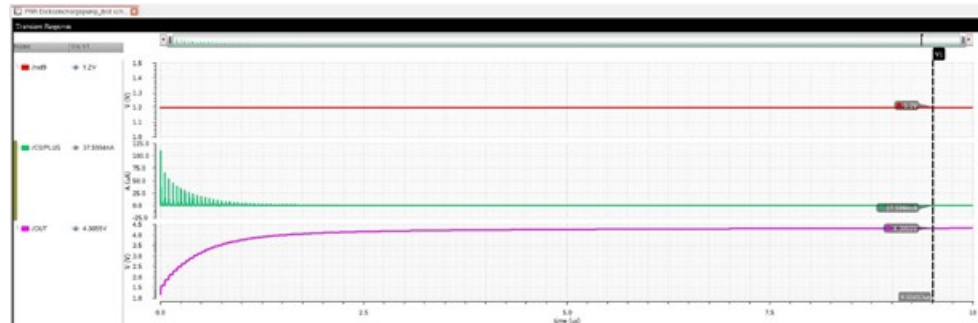


Figure 3.9: Transient analysis output of 4-stage Dickson charge pump

simulation purposes, an n type MOSFET of gpdk090 technology and a capacitor of 1 pF capacitance has been used. An N stage Dickson charge pump can be designed by cascading single stage charge pumps. A 4-stage charge pump is designed as given in Figure 3.8. Another n type MOSFET and a capacitor are used in series as a load. An input voltage source of 1.2 V and two voltage pulses of peak voltage 1.2 V are used as clock sources. Figure 3.9 gives the transient analysis output of the 4-stage Dickson charge pump. From the plots it is noted that the circuit produces an output voltage of 4.3055 V for an input voltage of 1.2 V. The voltage increases exponentially initially and saturates after a while. Figure 3.10: gives the DC analysis and power plot outputs of the 4-stage Dickson charge pump given in

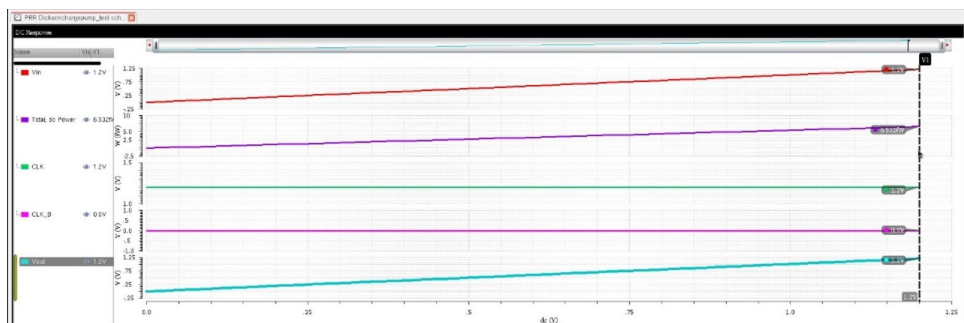


Figure 3.10: DC analysis and power plot outputs of 4-stage Dickson charge pump

Figure 3.8. The power plot increases linearly with time. It also depends on the load connected to the charge pump. DC plots of input voltage source are also plotted.

3.3 Cross Coupled Charge Pump

The circuit, Figure 3.11. is perfectly symmetrical and all the components have the same parameters. Two complementary clocks with amplitude V_{DD} are provided.

1. Working and Modelling: The operation of this charge pump topology can be divided into two phases. During phase1 clk is high and clk' is low, the opposite happens in phase 2 [13]. During phase 2, the nodes V_1 and V_2 are at $2V_{DD}$ and C_{DD} respectively,

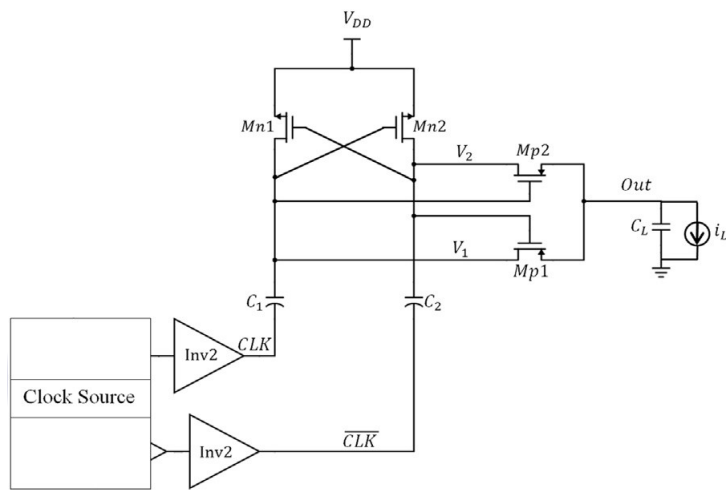


Figure 3.11: Single stage cross coupled charge pump with a clock source

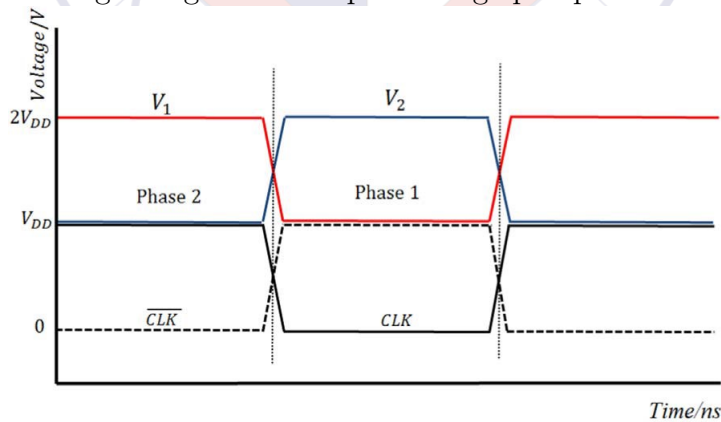


Figure 3.12: Timing diagram of cross coupled charge pump

M_{P1} is ON and M_{P2} is OFF and the output is at $2V_{DD}$. As the circuit enters phase1, CLK goes low and CLK' goes high. Node V_1 is discharged to V_{DD} turning M_{N2} OFF and node V_2 is boosted to $2V_{DD}$ turning M_{N1} ON. This sequence of events turns M_{P2} ON and M_{P1} OFF, thus the output is at $2V_{DD}$. In phase 2 the roles of M_{N1}

and M_{N2} are swapped, as well as the role of M_{P1} and M_{P2} , and thus the output sees a constant voltage of $2V_{DD}$. Figure 3.12 describes the complete procedure.

When the circuit enters phase1 CLK goes low, turning M_{N2} OFF. As CLK goes to V_{DD} , the charge stored in C_2 must be conserved as there is nowhere for the current/charge to flow out (because M_{N2} and M_{P2} are still OFF and there are no parasitics connected to node V_2). Thus the voltage at the top plate of C_2 is boosted up to $2V_{DD}$.

When assumed that there is no load or parasitic load, then it is found that the charge stored in capacitor C_2 during phase2 is given by equation (3.13).

$$Q_{ph2} = C_2 \times V_{DD} \quad (3.13)$$

Hence it is seen that during the complete time period of working, there is always $2V_{DD}$ voltage present at the output node of a single stage charge pump.

If parasitic capacitances at node V_2 are taken into account (coming from the top plate of C_2 , gate of M_P , M_{N1} and drains of M_P , M_{N2}) then some charge must flow to these parasitics in order to raise their voltage above V_{DD} . As M_{N2} and M_{P2} are OFF, this charge comes from C_2 which results in a charge loss and voltage reduction, as shown in Figure 3.13. The reduction in voltage (V_{lost}) and the current

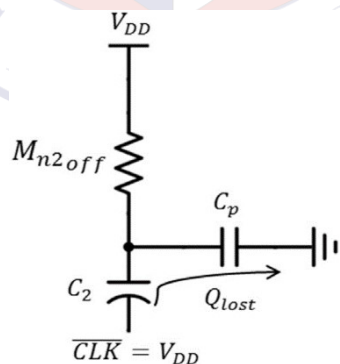


Figure 3.13: Circuit explaining the lost charge parasitics in phase 1

that flows to the parasitics can be represented as equation (3.14)

$$\begin{aligned} V_{lost} &= \frac{Q_{lost}}{C_2} \\ i_p &= C_p \frac{dV_2}{dt} \end{aligned} \quad (3.14)$$

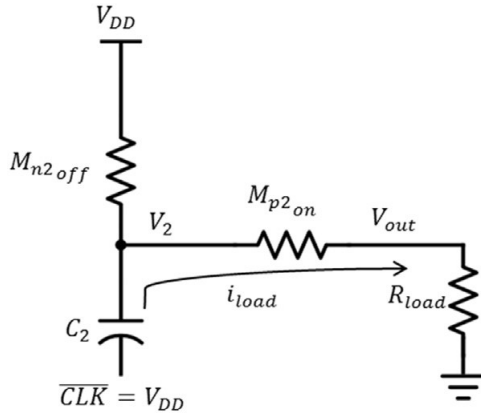


Figure 3.14: Half circuit modelled during phase 1 when load is connected

where i_p is the current that flows from C_2 to C_P in order to charge it up and dV_2/dt is the rate of change of voltage at node V_2 . Assuming that CLK' transitions from low-to-high in linear fashion, the voltage at node V_2 will transition in a linear fashion as well and thus:

$$i_p = C_p \times \frac{V_0 - V_{DD}}{T_r} \quad (3.15)$$

This equation (3.15) models the output voltage with time during the half period of the clock cycle. The final voltage the output settles at, $V_{out\text{-final}}$, as in equation (3.16).

$$V_{out\text{-final}} \approx \gamma V_{DD} - \frac{i_L}{2fC_2} \quad (3.16)$$

When a load current is connected at the output, the circuit can be modeled during phase 1 as shown in Figure 3.14. The circuit is perfectly symmetrical with $C_1 = C_2 = C$. The same equation as above is obtained on considering C_L equal to zero. Hence it can be seen that the final output voltage would be the same whether a load capacitor is connected to the output or not.[16]

2. Simulation:

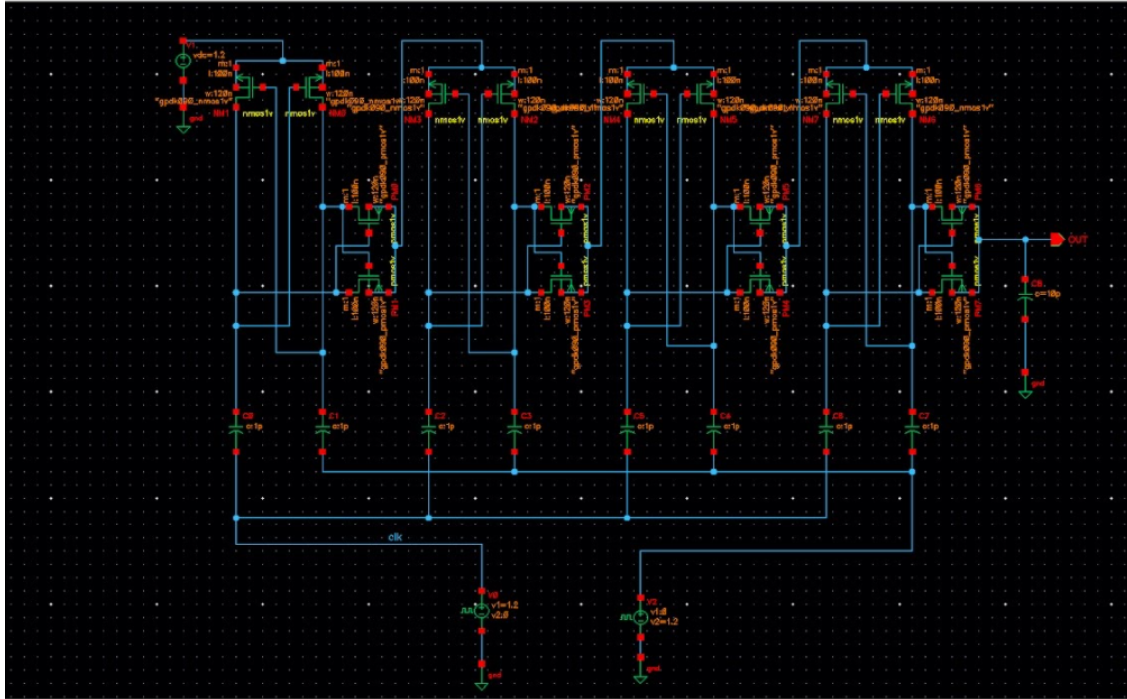


Figure 3.15: Four stage schematic of cross coupled charge pump in transistor level

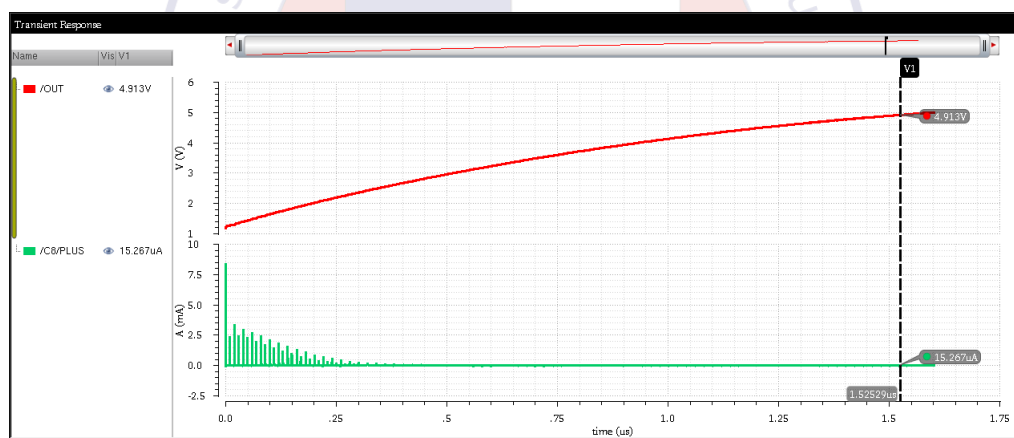


Figure 3.17: Transient response with current plot along with output voltage

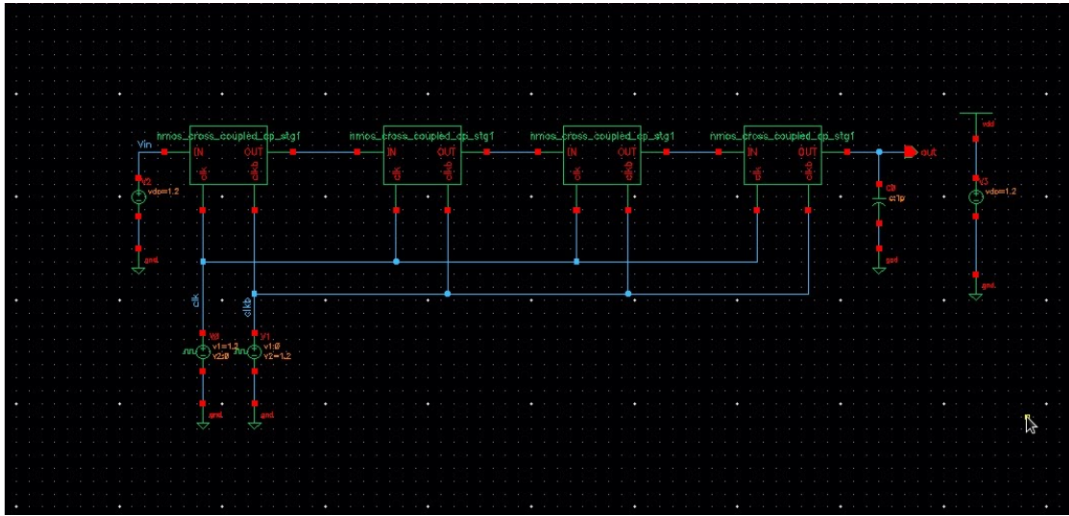


Figure 3.16: Block level schematic of four stage cross coupled charge pump

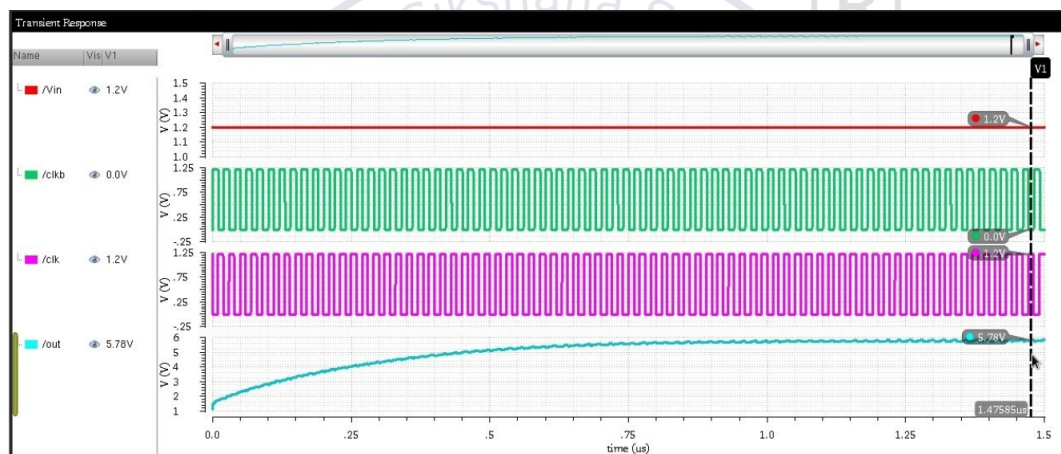


Figure 3.18: Transient analysis of output voltage after four stages

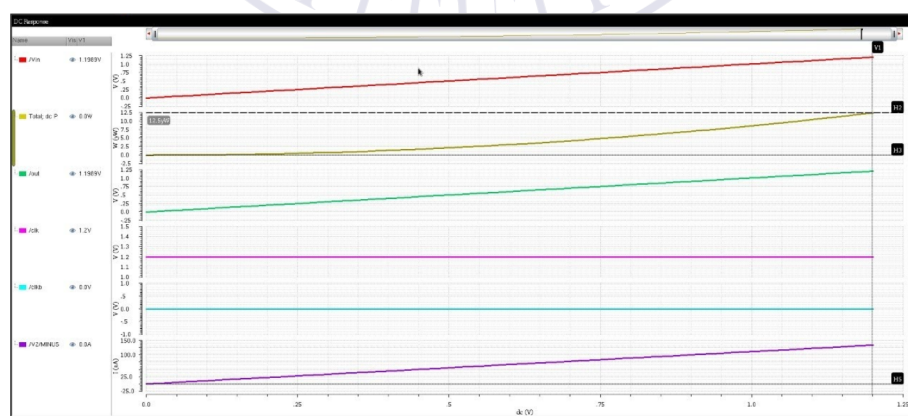


Figure 3.19: DC analysis of four stage cross coupled charge pump

Figure 3.15 and Figure 3.16 are the schematic of cross coupled charge pump transistor level and block level respectively. Simulations of the cross coupled charge pump

done on cadence virtuoso are presented. Figure 3.17 and Figure 3.18 represents the transient analysis of the cross coupled charge pump. Output voltage at the end of four stages is 5.78V. DC analysis is given by Figure 3.19.

3.4 Cross Coupled Charge Pump with Bulk Biasing

Body (or bulk) biasing techniques are applied to better manage the transistor during on and off phases and to improve its electrical properties, such as threshold voltage and on/off resistance. This topology is proposed for low voltage operation. The charge pump with an integrated ring oscillator has sub-threshold operation and body bias technique to enable startup and operation under a low voltage supply as in equation (3.17).

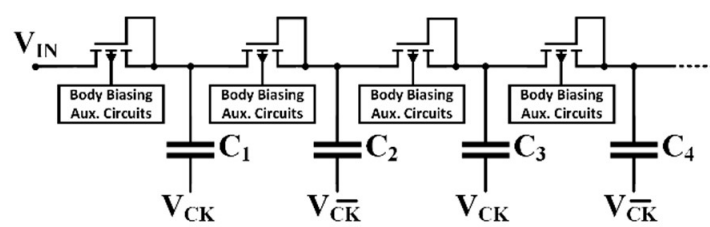


Figure 3.20: Generalised circuit for body biasing technique

1. Working: The Figure 3.20 shows the topology usually employed for low voltage applications and is obtained using the body effect phenomenon. Body effect is the change in the threshold voltage of a transistor due to the difference in voltage between the source and bulk terminals of the transistor.

$$V_{TH} = V_{T0} + \gamma \left(\sqrt{2|\phi_F| + V_{SB}} - \sqrt{2|\phi_F|} \right) \quad (3.17)$$

This threshold is technology specific and the transistor does not work when the gate voltage is lower than the threshold. Hence there is always a minimum drop of voltage equal to the threshold voltage to be covered by the input signal. To avoid this drop, the source-bulk voltage is varied to reduce the threshold voltage and make the transistor operable in low voltage applications [17].

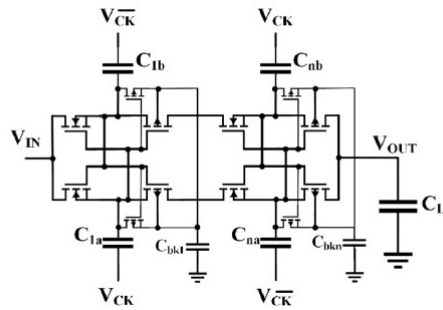


Figure 3.21: Single Stage Cross coupled CP with Bulk Switching

As seen in the Figure 3.21, PMOSs are body biased using transistors. This has been done to help with low power applications.

2. Simulation:

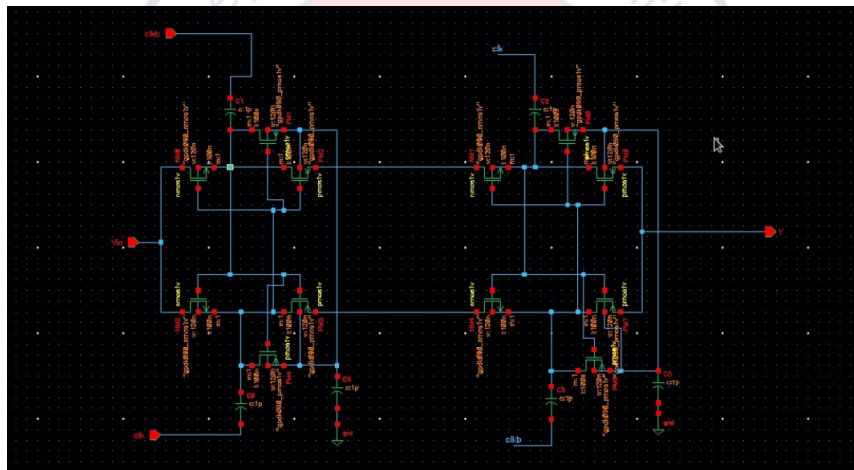


Figure 3.22: Schematic of single stage

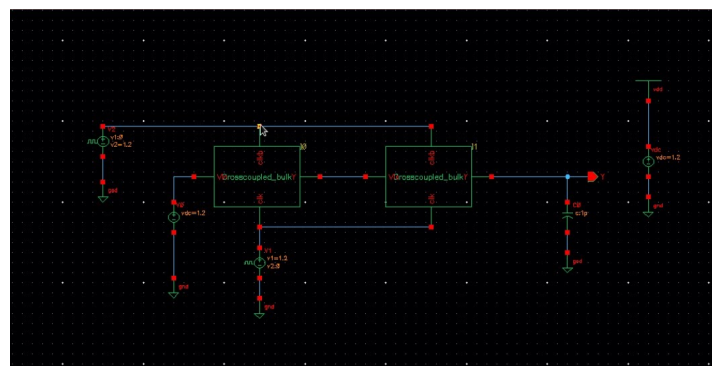


Figure 3.23: 2 stage Cross Coupled CP with Bulk Biasing block diagram

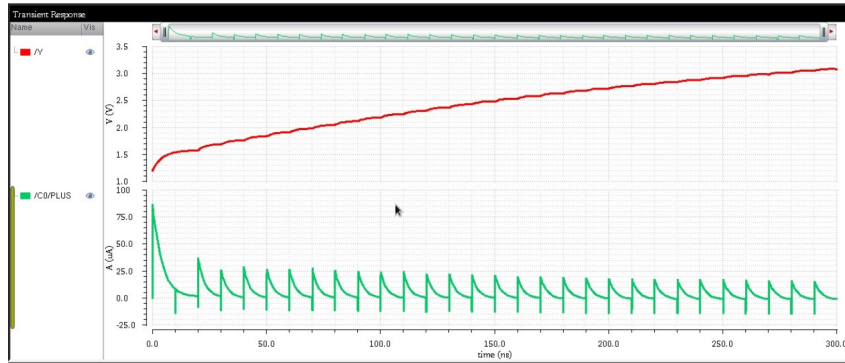


Figure 3.24: Transient Analysis with Current plot and output voltage

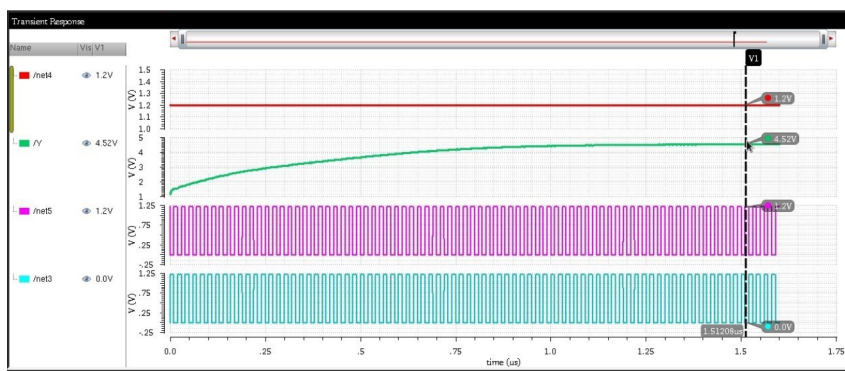


Figure 3.25: DC analysis of with output voltage

Figure 3.25 and Fig 3.22 represent the single stage schematic of Cross Coupled Charge Pump with Bulk Bias and 2 stage cascaded implementation of the same, respectively.

3.5 Comparison

Table 3.1: Comparison of charge pump topologies

Charge pump topology	Number of stages	Total no. of transistors	Output voltage considering no load
Dickson CP	4	4	4.3055V
Cross coupled CP	4	16	5.78V
Cross coupled with bulk bias CP	2	24	4.52V

From Table 3.1 it is inferred that the Dickson charge pump requires the least number of transistors for a four stage topology. The output voltage at the end of four stages is highest in the case of the cross coupled charge pump. The cross coupled with body

biasing has comparatively more number of transistors used, and as the fourth terminal is also being engaged, hence it has to be fabricated using the twin-well process. In case of Dickson charge pump, as the number of pumping stages is increased the output voltage decreases due to the body effect of the diode connected NMOS transistor. The pumping efficiency decreases as the number of stages increases.

The comparison shows that the cross coupled charge pump provides improvements in terms of output voltage, power consumption. Therefore, the cross coupled charge pump topology is chosen for the application based on its better performance over others.

The fourth chapter presents the additional circuitry required for the operation of the final integrated circuit. The OTA, oscillator and battery circuits are discussed in detail along with their simulation results.





Chapter 4

ADDITIONAL CIRCUITS: OPERATIONAL TRANSCONDUCTANCE AMPLIFIER, OSCILLATOR AND BATTERY CIRCUIT

CHAPTER 4

ADDITIONAL CIRCUITS: OPERATIONAL TRANSCONDUCTANCE AMPLIFIER, OSCILLATOR AND BATTERY CIRCUIT

In order to charge the battery a few additional circuitry and signal conditioning circuits are required. This chapter mainly focuses on the additional circuits made use of in the integrated design. Operational transconductance amplifier, oscillator and battery circuits are discussed in detail.

4.1 Operational Trans-conductance Amplifier

The main challenge that is faced while processing the output signal of the charge pump, is the low current in that signal, this challenge can be overcome using an OTA (operational transconductance amplifier). The OTA is very much similar to an opamp. The OTA behaves like a voltage controlled current source. Unlike the opamp the output impedance of an OTA approaches infinity. This can be best used to describe the forward gain. Its basic operation is like a differential amplifier with noise cancellation properties. It also has a capacitive load, which acts as a short circuit and helps in filtering the high frequency noises. The performance of the OTA impacts the overall power consumption and voltage gain.

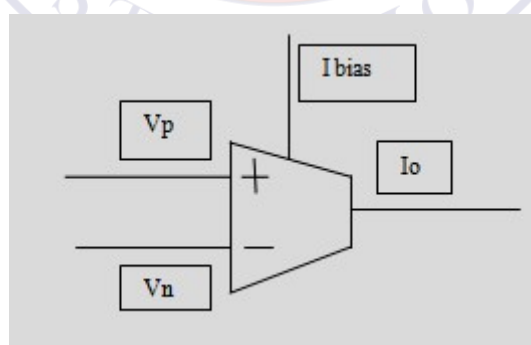


Figure 4.1: Ideal OTA model

Figure 4.1 describes the ideal OTA model, V_P and V_N represent the positive and negative inputs respectively, I_{BIAS} is the external current source, and I_0 is the output current. The output current I_0 is the resultant of the input voltages V_P and V_N .

The output current of the OTA can be defined by the equation (4.1).

$$I_o = G_m \times (V_p - V_n) \quad (4.1)$$

where, G_m = transconductance of the amplifier.

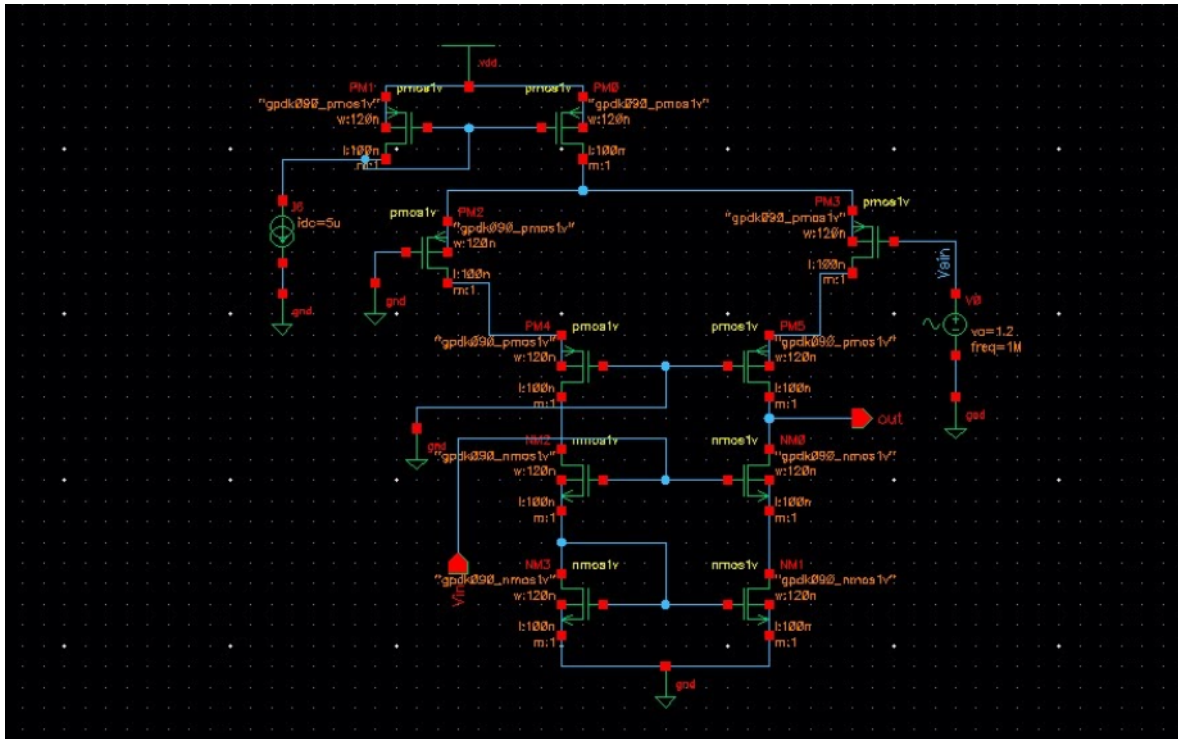


Figure 4.2: Schematic of the OTA

The circuit in Figure 4.2 represents the circuit diagram of the OTA in the telescopic configuration. The inputs in this configuration can be given as a differential input, but in order to simplify it, only the positive input terminal is made use of, and the negative terminal is grounded. If a set of transistors are operating in the saturation mode as a transistor pair, then one leg of the transistors will turn on at a particular time while turning the other off. From one leg the current will sink from the load while the current will be sourced to the output from the other leg. The differential input is applied across the gate of P_{M2} and P_{M3} . An external DC source is used in order to control the transconductance of the amplifier. The transistors in this configuration are arranged in a stacked manner one on top of the other which enhances the output impedance and thus the gain. This OTA also provides lower power consumption and a higher speed.[18] Figure 4.3 provides the transient response of the OTA, with an input voltage of 5.8V. From the

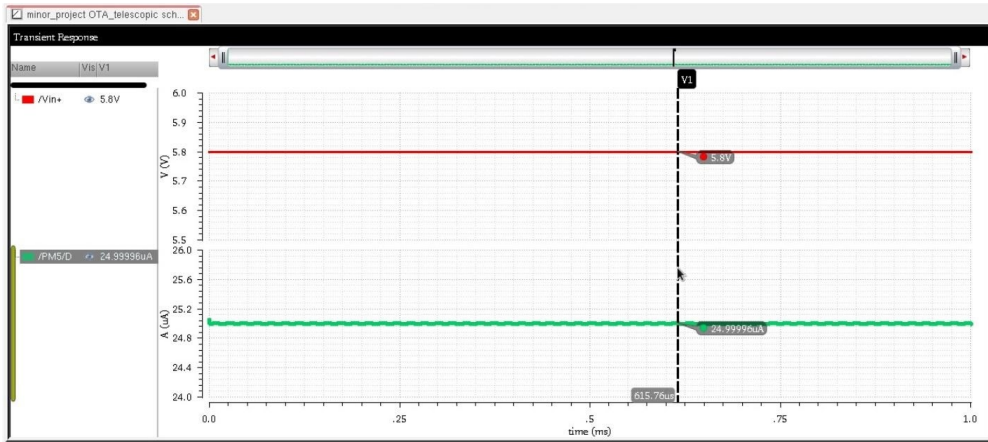


Figure 4.3: Transient response of the OTA

graph it can be interpreted that the output current is $24.99\mu\text{A}$. Cascode configuration of OTA is made use of in the integrated design as it is an improvised version of an OTA when compared to the current mirror and single stage cascode configurations.

4.2 Oscillator

For the simplicity of the NOT gate based oscillator, it has been used in this application. The ring oscillator outputs are used to provide the positive and negative clock source to the charge pump. Figure 4.4. is the schematic of the oscillator used in the design. Three NOT gates are used with feedback to function as an oscillator. This ring oscillator drives the gate of the MOSFET through buffers. Two nodes are used to connect V_{DD} and ground. The output of the oscillator as shown in Figure 4.5 has a frequency of 13.9

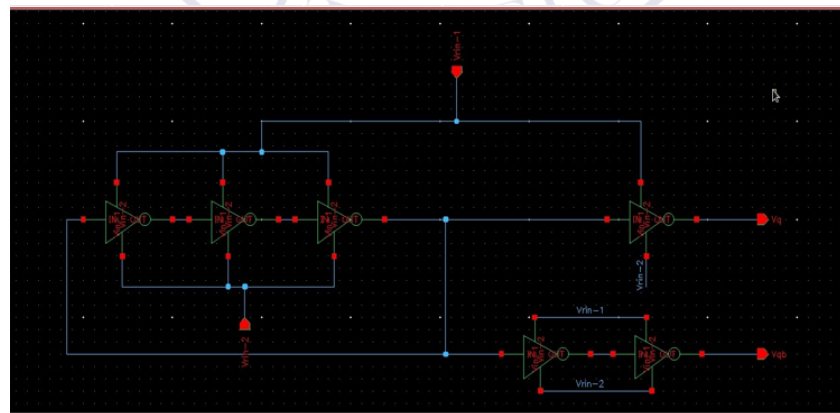


Figure 4.4: Ring oscillator with buffers

GHz. The simulations are carried out on the Cadence Virtuoso tool using the components available in the gpdk090 component library.[19]

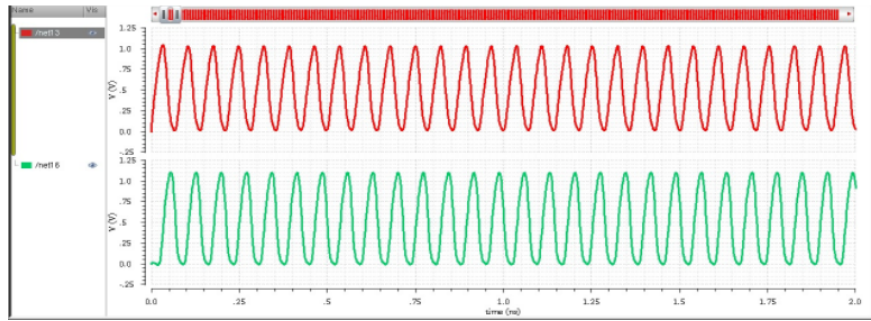


Figure 4.5: Output of the oscillator

4.3 Battery Circuit

The battery used in the pacemaker device needs to be recharged on a regular basis thereby making it work continuously and keep the patient stable. The energy for recharging is harvested from the nearby harvesting sources like radio frequency (RF), solar, thermal, flow-based, and vibration energy present within or near the body [2]. To study this charging and discharging process of the battery, a proper model needs to be designed which physically represents the battery functioning perfectly. The modeled battery must be able to provide all the necessary details like impedance, open circuit voltage, current and state of charge(SOC) of the battery. State of charge is the relative level of charge with respect to its capacity. This is one of the important parameters in understanding battery performance. The SOC is determined by the Ampere-counting method where the biasing of the charge that is transferred into the battery is taken out of the battery. The SOC is a function of the open circuit voltage (OCV) of a lithium-ion battery, $SOC=f(OCV)$ but it faces problems in dynamics [20]. The OCV can't be measured at the terminals of the battery during the electrochemical process taking place within the cell. Variables need to be mathematically performed in such a way that the OCV sequence SOC can only be calculated by measuring the current and battery voltage in the battery terminals. For this purpose an equivalent circuit diagram of the battery cell must be used, and the parameters should be identified by the feature dimensions. The state of charge is modeled as shown in Figure 4.6. satisfying the required conditions that is a function of open circuit voltage.

The physical Li Ion rechargeable battery performance, used in the pacemaker device, is modeled in the following ways [21]

1. IR Model: The battery is modeled as shown in Figure 4.7 where the ideal voltage

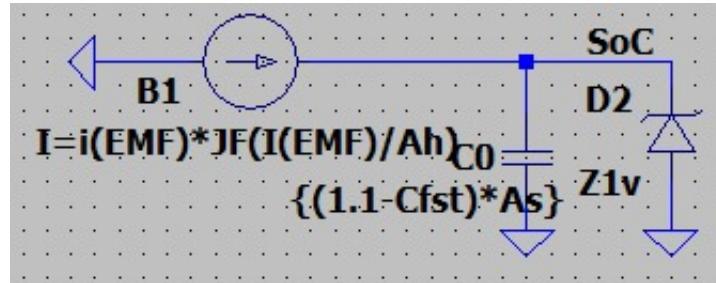


Figure 4.6: State of Charge Model

source V represents the open circuit voltage of the battery and the rest representing the internal impedance of the battery. Both the resistance and the open circuit voltage are the functions of the SOC, state of health (SOH) and temperature. The current discharging from the battery is positive and the terminals A_{POS} and A_{NEG} represent the two terminals of the battery.

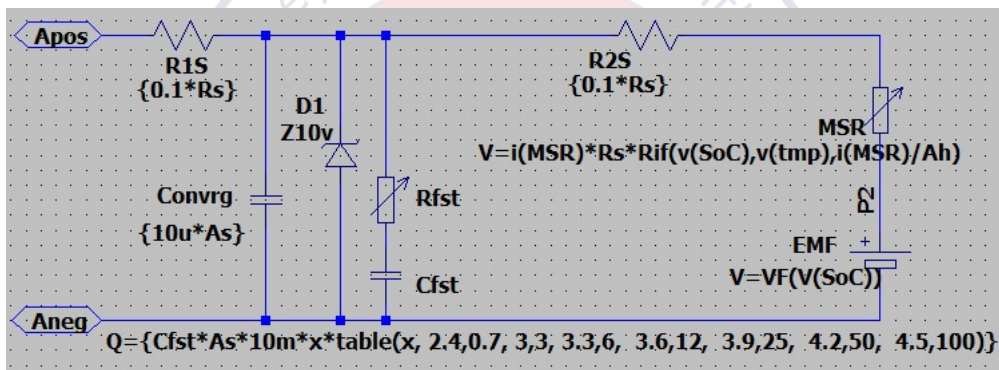


Figure 4.7: The IR Model of Rechargeable Li Ion Battery

The IR model fails to represent the transient behavior of the Li Ion battery used and it is not suitable for correct determination of the SOC during non constant load.

2. TTC Model: Two Time Constant model adds a parallel RC network in series with the internal resistance of the IR model therefore approximating the varying behaviour of the lithium ion battery. Two parallel RC networks are added in series to the IR model to improve it's flexibility and reduce the difference between short time and long time transient behaviour, which means accurately modeling the varying behaviour of the rechargeable Li Ion battery. Figure 4.8 represents the TTC model of the Li Ion battery where voltage source V_{OCC} , internal resistance of the battery R_O , V_{TTC1} represent the voltage drop across the first parallel RC network, V_{TTC2}

represent the voltage drop across the second parallel RC network, $R_{TTC1}(R_2)$ and $C_{TTC1}(C_2)$ describe the short term characteristics and $R_{TTC2}(R_3)$ and $C_{TTC2}(C_3)$ describe the long term characteristics of the battery modeled with I_{TTC1} and I_{TTC2} current flowing through the capacitors $C_{TTC1}(C_2)$ and $V_{TTC2}(C_3)$.

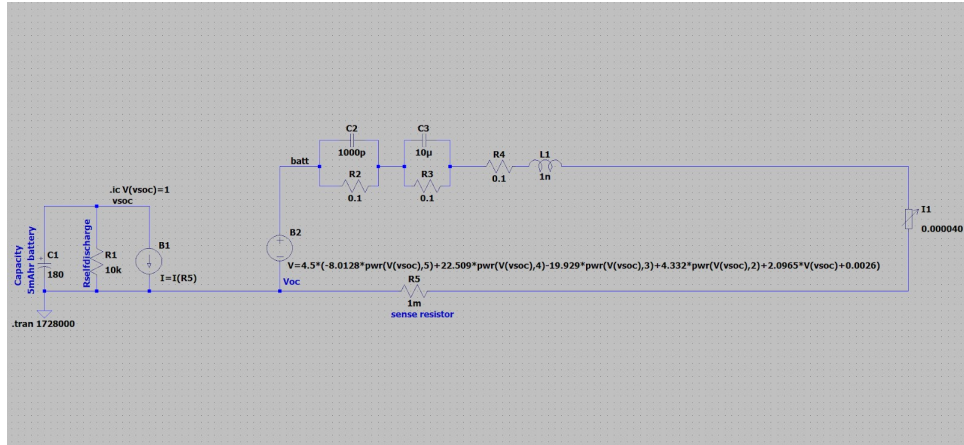


Figure 4.8: The IR Model of Rechargeable Li Ion Battery

The TTC circuits electrical behaviour is expressed in following Equation (4.2), (4.3), (4.4) in continuous time:

$$\dot{v}_{TTC1} = \frac{-1}{C_{TTC1}R_{TTC1}}v_{TTC1} + \frac{1}{C_{TTC1}}i_{Batt} \quad (4.2)$$

$$\dot{v}_{TTC2} = \frac{-1}{C_{TTC2}R_{TTC2}}v_{TTC2} + \frac{1}{C_{TTC2}}i_{Batt} \quad (4.3)$$

$$v_{Batt} = V_{OC} - v_{TTC1} - v_{TTC2} - R_0 i_{Batt} \quad (4.4)$$

The behaviour in discrete time sequence is represented by Equation (4.5), (4.6), (4.7)

$$v_{TTC1,k+1} = v_{TTC1,k} e^{\frac{-T_S}{\tau_{TTC1}}} + R_{TTC1} \left(1 - e^{\frac{-T_S}{\tau_{TTC1}}} \right)_{i_{Batt,k}}, \quad (4.5)$$

$$v_{TTC2,k+1} = v_{TTC2,k} e^{\frac{-T_S}{\tau_{TTC2}}} + R_{TTC2} \left(1 - e^{\frac{-T_S}{\tau_{TTC2}}} \right)_{i_{Batt,k}}, \quad (4.6)$$

$$v_{Batt,k} = V_{OC}(SOC_k) - v_{TTC1,k} - v_{TTC2,k} - R_0 i_{Batt} \quad (4.7)$$

Estimation of TTC Model: From Figure 4.9, during the subinterval $S2(t1 \leq t \leq t2)$ and $S4(t \geq t3)$, the battery output current $i_{BATT} = 0$ and battery output voltage will have a steep increase/ decrease due to R_o (internal resistance of the battery) and it exponentially increases/ decreases until it reaches $VOC(SOC1)$ and $VOC(SOC2)$ respectively.

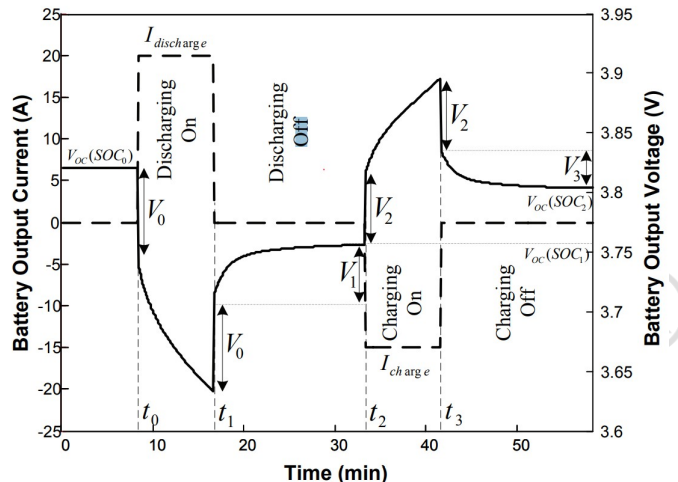


Figure 4.9: Li Ion battery's Characteristics waveform for battery voltage and current during charging and discharging

As in these sub intervals S_2 and S_4 OCV is constant, the output voltage of the battery is driven by dynamic characteristics of the battery and its value is calculated by equating $i_{BATT} = 0$ and differentiating Equation (4.2), (4.3), (4.4). The TTC model output voltage can be expressed as

$$\begin{cases} \tau_{TTC1} = R_{TTC1} C_{TTC1} \\ \tau_{TTC2} = R_{TTC2} C_{TTC2} \end{cases} \quad (4.9)$$

The identification of TTC model requires to determine the parameters $\text{VOC}(\text{SOC}1)$, $\text{VOC}(\text{SOC}2)$, $V_{\text{TTC}1}(t_1)$, $V_{\text{TTC}1}(t_3)$, $V_{\text{TTC}2}(t_1)$, $V_{\text{TTC}2}(t_3)$, TTC_1 and TTC_2 from Equation (4.8) and (4.9) which looks similar to that of two time constant function $f(t) = A + Be^{-\alpha t} + Ce^{-\beta t}$. The coefficient vector A , B , C , α , and β obtained

from the non linear least square algorithm can be used to calculate the TTC model parameters as in eqation (4.10), (4.11), (4.12) and (4.13).

$$\left\{ \begin{array}{l} S_2 : V_{OC}(SOC_1) = A \\ S_4 : V_{OC}(SOC_2) = A \end{array} \right. \left\{ \begin{array}{l} S_2 : v_{TTCl}(t_1) = B, v_{TTC2}(t_1) = C \\ S_4 : v_{TTCl}(t_3) = B, v_{TTC2}(t_3) = C \end{array} \right. \quad (4.10)$$

$$\left\{ \begin{array}{l} \tau_{TTC1} = \frac{l}{\alpha} \\ \tau_{TTC2} = \frac{1}{\beta} \end{array} \right. \quad (4.11)$$

$$\left\{ \begin{array}{l} S_2 : R_{TTC1} = \frac{v_{TTC1}(t_1)}{\left(1-e^{-\frac{T_{\text{discharge}}}{\tau_{TTC1}}}\right)I_{\text{discharge}}} \\ S_4 : R_{TTC1} = \frac{v_{TTCl}(t_3)}{\left(1-e^{-\frac{T_{\text{charge}}}{\tau_{TTC1}}}\right)I_{\text{charge}}} \end{array} \right. \left\{ \begin{array}{l} S_2 : R_{TTC2} = \frac{v_{TTC2}(t_1)}{\left(1-e^{-\frac{T_{\text{discharge}}}{\tau_{TTC2}}}\right)I_{\text{discharge}}} \\ S_4 : R_{TTC2} = \frac{v_{TTC2}(t_3)}{\left(1-e^{-\frac{T_{\text{charge}}}{\tau_{TTC2}}}\right)I_{\text{charge}}} \end{array} \right. \quad (4.12)$$

$$\left\{ \begin{array}{l} C_{TTCl} = \frac{\tau_{TTC1}}{R_{TTC1}} \\ C_{TTC2} = \frac{\tau_{TTC2}}{R_{TTC2}} \end{array} \right. \quad (4.13)$$

The discharge curve of the TTC model Li Ion battery of voltage capacity of 4.5 Volts and the output load drawing a constant current of 40 μ Ampere is being simulated which is generally used in the pacemaker devices. It is noted that the battery voltage drops very slowly and takes 1.8 Million seconds to drop the battery voltage from 4.5 Volts to 1.4 Volts as shown in Figure 4.10. A similar discharge curve of Li Ion battery is plotted for different battery voltages and output current loads as shown in Figure 4.12.

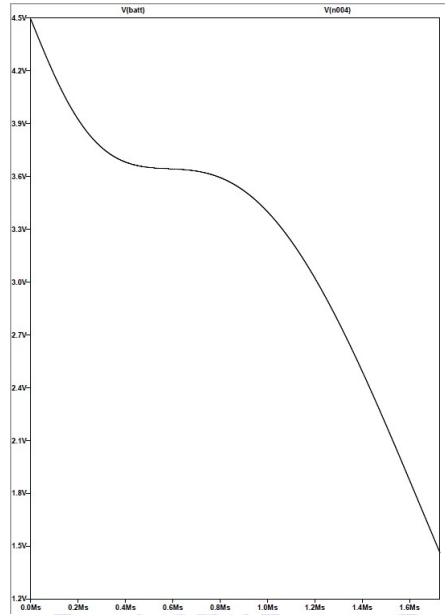


Figure 4.10: Discharge Curve of TTC Model Li Ion Battery

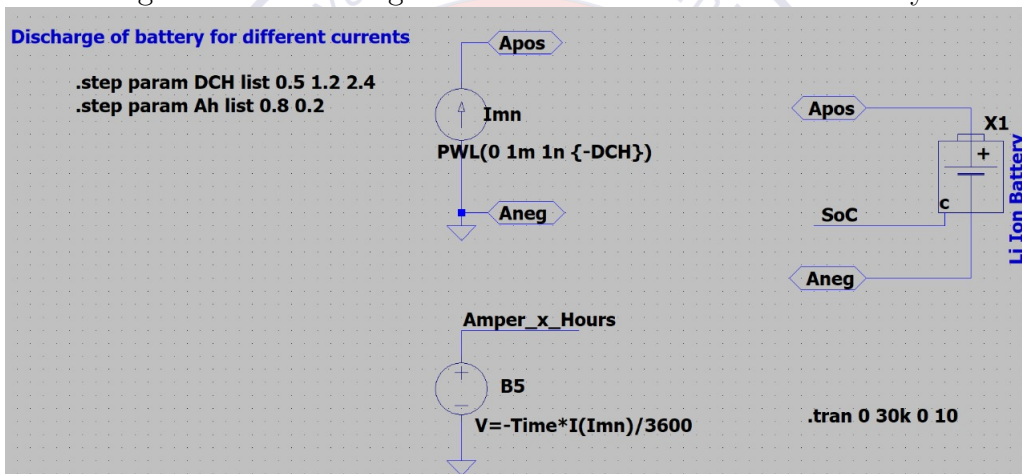


Figure 4.11: Discharge of Li Ion Battery Model for Different load currents

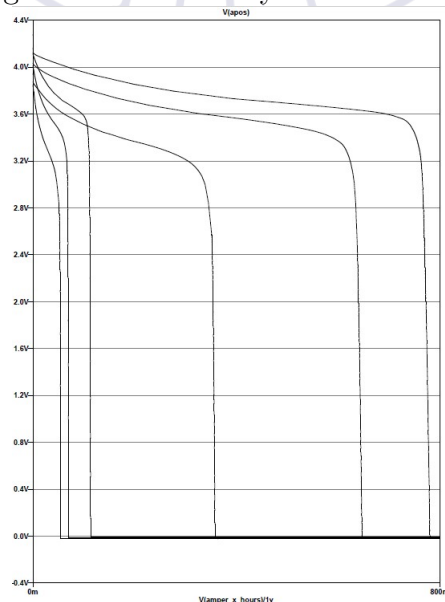


Figure 4.12: Output of Discharge of Li Ion Battery for Different load currents

Two Li Ion batteries models of capacity 800 mAh and 200 mAh are connected in series as shown in Figure 4.13. A constant current pulse of period 20 kilo seconds is applied as shown in Figure 4.14. During the negative half cycle the battery is discharged from its maximum voltage at constant current and in the positive half cycle the battery is charged at a constant current. The battery with least capacity gets charged and discharged faster than the battery with highest capacity as shown in Figure 4.15. The battery's SOC is detected at 18 kilo seconds by providing a dc voltage of 0.5V for a short period of time. During this period the battery is charged to almost half of its capacity. Figure 4.16 shows the relative SOC of the battery over a scale of 0.0V to 1.0V indicating the no charge and full charge of the battery.

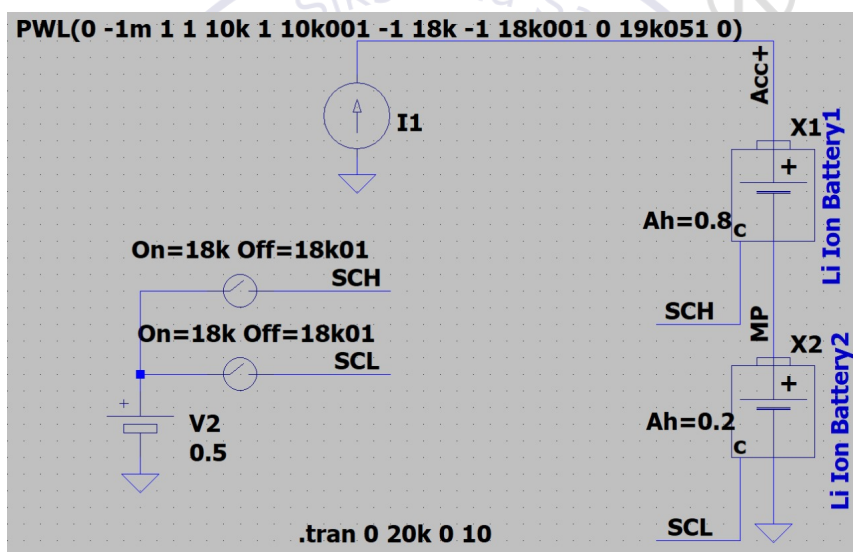


Figure 4.13: Charging and discharging of Li Ion Battery Model

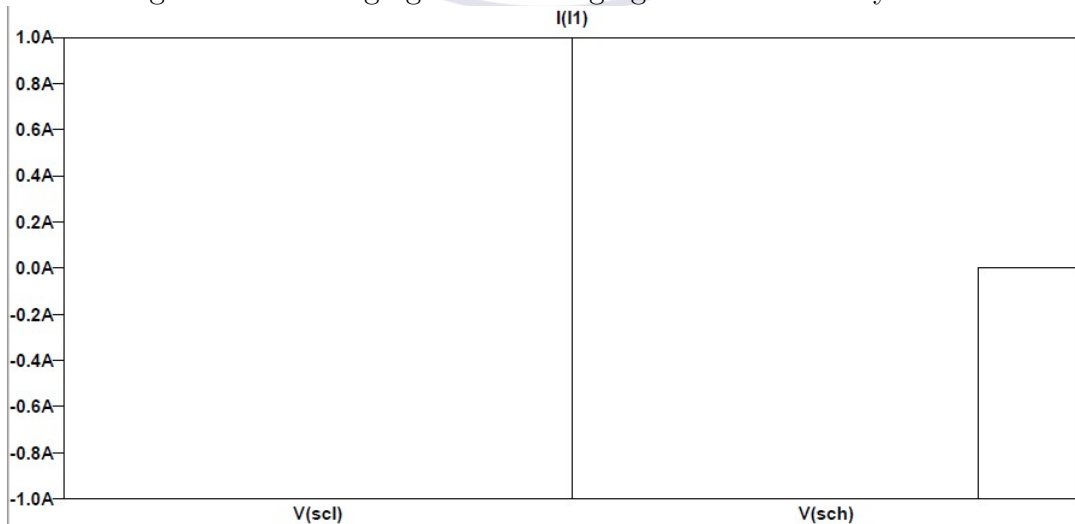


Figure 4.14: Input Current Pulse

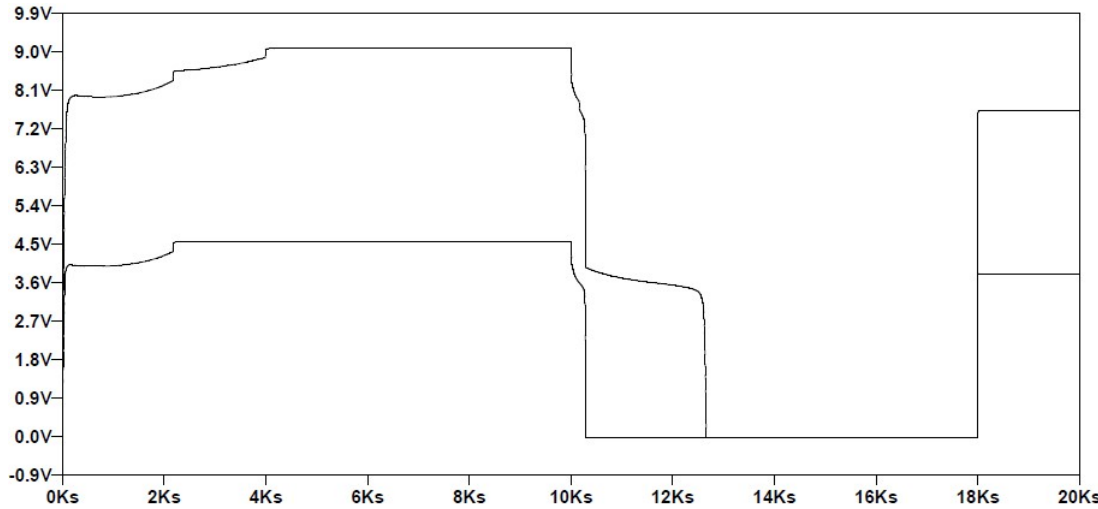


Figure 4.15: Battery voltage level with time

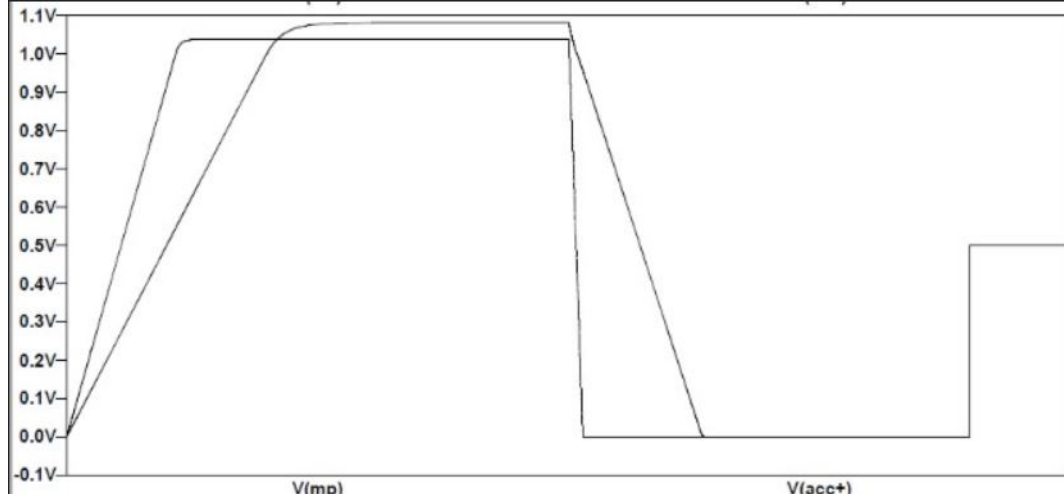


Figure 4.16: State of Charge of the Battery

The detailed analysis of the Operational transconductance amplifier, oscillator and the battery circuit was dealt with in this chapter. The operational transconductance amplifier and oscillator were simulated using the Cadence Virtuoso tool. Battery modelling was done using the LTspice tool. The next chapter deals with the working, design and simulation of the integrated circuit.



Chapter 5

Results & Discussion

CHAPTER 5

RESULTS & DISCUSSION

The charge transfer circuit is designed by choosing the most appropriate schematics based on performance, size and power consumption and integrating it with the additional circuits required for functioning of overall design. This chapter explains the interfacing and functioning of the integrated circuit. Simulation results are also explained.

5.1 Integrated circuit

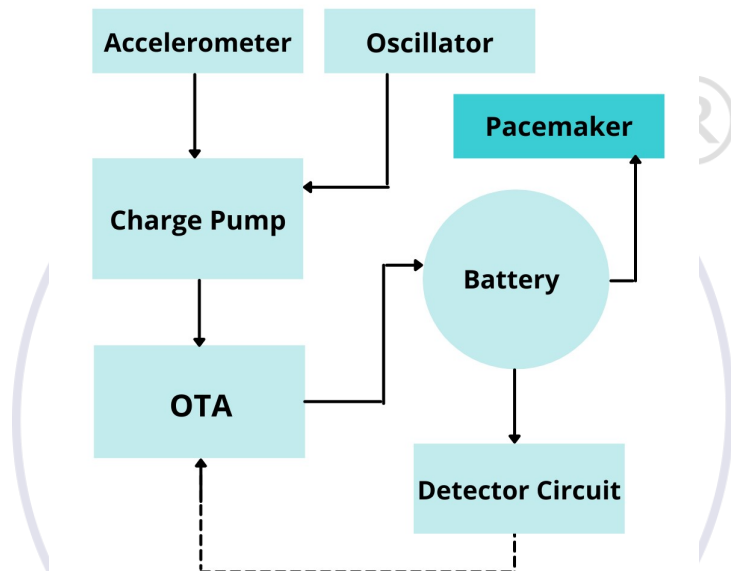


Figure 5.1: Block diagram representation of the integrated circuit

The designed and implemented integrated circuit consists of multiple blocks which are a charge pump, operational transconductance amplifier (OTA) and an oscillator as shown in Figure 5.1. The output voltage from the accelerometer is given as the input to the charge pump. The oscillator is used as the clock source to make the charge pump operational. In order to charge the battery, a constant current is required. The output voltage from the charge pump is provided as a differential input to the OTA, which is a voltage controlled current source. A constant current is available at the output of the OTA, which is used to charge the lithium ion battery in the constant current mode. A detector circuit, which is optional, is used to detect the state of charge of the battery and to put the rest of the circuitry into sleep mode. Using this proposed setup, the lithium ion battery is charged and the pacemaker is powered.

5.2 Simulation of the integrated circuit

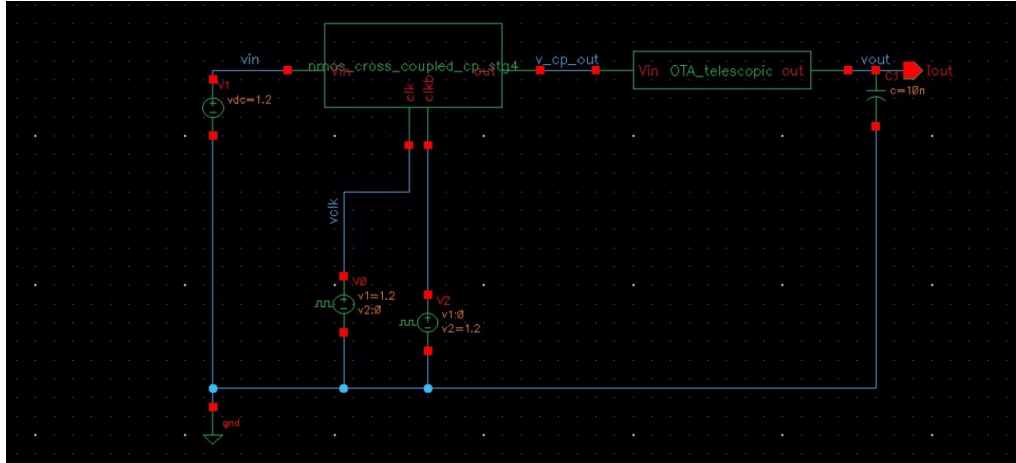


Figure 5.2: Schematic diagram of the integration of cross coupled charge pump with OTA

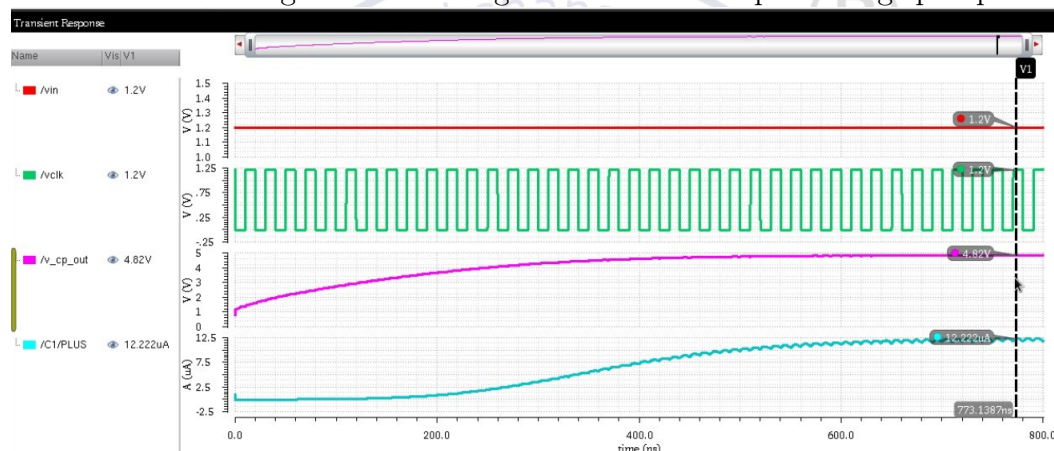


Figure 5.3: Transient response of the integrated circuit

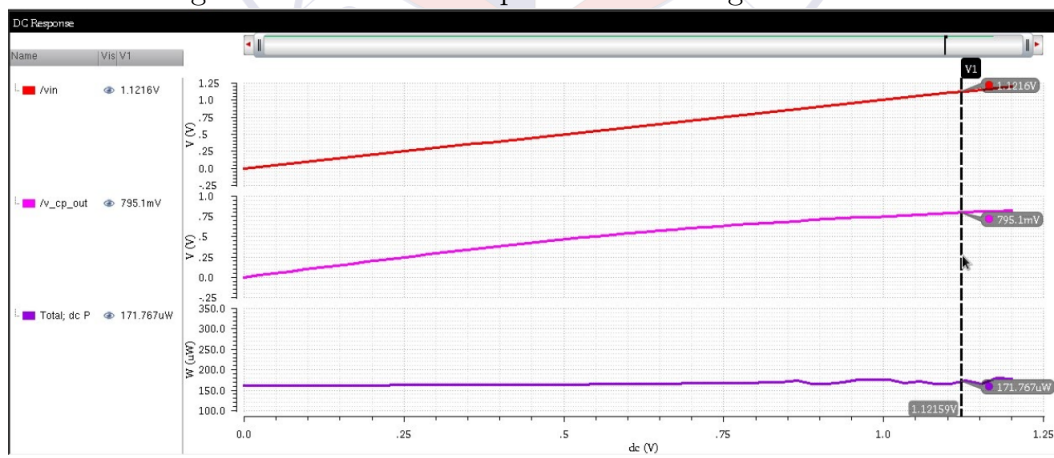


Figure 5.4: DC response of the integrated circuit with power plot

As the simulation of the battery is done in LTspice simulation software, the integrated circuit in Figure 5.2. only includes the components which could be designed on Cadence Virtuoso. Cross coupled charge pump is made use of in the integrated circuit due to

it's advantages over the other topologies of charge pumps. Figure 5.2. Is the transient response of the integrated circuit. Given the input voltage of 1.2V and a constant clock signal from the oscillator, voltage available at the output of the charge pump is seen to be 4.82 V. This value is degraded because the OTA is acting as a load on the charge pump. The current at the output of the OTA is found to be 12.22 uA. The current available is almost constant and can be used to charge the Li-ion battery. Figure 5.4. shows the power plot of the integrated circuit and the peak power is found to be 171.76 uW.

This chapter discussed the proposed integrated circuit sufficiently. The following chapter gives a brief conclusion of all the chapters discussed until now and also some of the few areas or topics in which further work can be carried out in order to improve the existing circuit.





Chapter 6

Conclusion and Future Scope

CHAPTER 6

CONCLUSION AND FUTURE SCOPE

6.1 Conclusion

The designed integrated circuit efficiently performs the charging of the battery using a charge pump and an operational transconductance amplifier as the main components. The charge pump takes input voltage from a harvesting element and gives an amplified output voltage to the operational transconductance amplifier which is a voltage controlled current source. The output voltage of the cross coupled charge pump is 5.83 V in no load condition and 4.82 V when a load is connected, which in this case is the operational transconductance amplifier. The output current of the operational transconductance amplifier is 12.22 uA constant current which is used for charging the battery. An additional stage of charge detection circuit can be added to the proposed integrated design in order to prevent the overcharging of the battery.

6.2 Future Scope

- Use of Depletion MOSFETs for self startup: The transistors used in all the circuits are enhancement MOSFETs. These MOSFETs have a positive threshold voltage requirement. In order to implement the circuits in self-startup conditions, there is a need for depletion mode MOS transistors which have a negative or zero threshold voltages and hence would be excellent in this application as very little input is required.
- Reduce the number of transistors in bulk biasing topology: The bulk biasing topology as discussed has a high number of transistors in a single stage which occupies more space even after having high output voltage from a single stage. A study on reducing the number of transistors in a single stage can be carried out.
- Circuit design considering the practical scenarios: The circuit proposed is designed considering ideal conditions i.e. the voltage fed into the charge pump from the accelerometer is considered to be regulated and constant, but considering the practical scenario there are a lot of variations. All the possible practical scenarios must be considered and the circuit has to be modified accordingly.

- Addition of Matching networks: In order to get the required results, impedance matching is essential. Matching networks can be designed for the integration wherever required for impedance matching to get the desired outcomes.
- Efficient battery design, considering bio-medical applications: Non toxic battery chemistry has to be chosen as the battery is embedded inside the human body. The battery should dissipate less power so that the charging and additional circuitry remains functional and efficiently carries out the operations.

6.3 Learning Outcomes of the Project

- Analyze and implement knowledge from various research publications and inculcate good research papers analyzing habits.
- Learn about various topologies of charge pumps and their applications.
- Learn to implement circuits and carry out simulations in Cadence Virtuoso
- Learn to prototype circuits in LTspice.
- Understand modelling of Li-ion battery

BIBLIOGRAPHY

- [1] D. Spillman and E. Takeuchi, "Lithium ion batteries for medical devices," in *Fourteenth Annual Battery Conference on Applications and Advances. Proceedings of the Conference (Cat. No.99TH8371)*, 1999, pp. 203–208. DOI: [10.1109/BCAA.1999.795991](https://doi.org/10.1109/BCAA.1999.795991).
- [2] E. O. Torres and G. A. Rincon-Mora, "Electrostatic energy-harvesting and battery-charging cmos system prototype," *IEEE Transactions on Circuits and Systems I: Regular Papers*, vol. 56, no. 9, pp. 1938–1948, 2009. DOI: [10.1109/TCSI.2008.2011578](https://doi.org/10.1109/TCSI.2008.2011578).
- [3] A. Zurbuchen, A. Haeberlin, A. Pfenniger, L. Bereuter, J. Schaerer, F. Jutzi, C. Huber, J. Fuhrer, and R. Vogel, "Towards batteryless cardiac implantable electronic devices—the swiss way," *IEEE Transactions on Biomedical Circuits and Systems*, vol. 11, no. 1, pp. 78–86, 2017. DOI: [10.1109/TBCAS.2016.2580658](https://doi.org/10.1109/TBCAS.2016.2580658).
- [4] C. Xiao, D. Cheng, and K. Wei, "An lcc-c compensated wireless charging system for implantable cardiac pacemakers: Theory, experiment, and safety evaluation," *IEEE Transactions on Power Electronics*, vol. 33, no. 6, pp. 4894–4905, 2018. DOI: [10.1109/TPEL.2017.2735441](https://doi.org/10.1109/TPEL.2017.2735441).
- [5] B. Do Valle, C. T. Wentz, and R. Sarpeshkar, "An area and power-efficient analog li-ion battery charger circuit," *IEEE Transactions on Biomedical Circuits and Systems*, vol. 5, no. 2, pp. 131–137, 2011. DOI: [10.1109/TBCAS.2011.2106125](https://doi.org/10.1109/TBCAS.2011.2106125).
- [6] B. D. Valle, C. T. Wentz, and R. Sarpeshkar, "An ultra-compact and efficient li-ion battery charger circuit for biomedical applications," in *Proceedings of 2010 IEEE International Symposium on Circuits and Systems*, 2010, pp. 1224–1227. DOI: [10.1109/ISCAS.2010.5537287](https://doi.org/10.1109/ISCAS.2010.5537287).
- [7] C. Liu, C. Jiang, J. Song, and K. T. Chau, "An effective sandwiched wireless power transfer system for charging implantable cardiac pacemaker," *IEEE Transactions on Industrial Electronics*, vol. 66, no. 5, pp. 4108–4117, 2019. DOI: [10.1109/TIE.2018.2840522](https://doi.org/10.1109/TIE.2018.2840522).

- [8] L. Wong, S. Hossain, A. Ta, L. Weaver, G. Shaquer, A. Walker, J. Edvinsson, D. Rivas, H. Naas, A. Fawzi, A. Uhrenius, J. Lindberg, J. Johansson, and P. Arvidsson, “A very low power cmos mixed-signal ic for implantable pacemaker applications,” in *2004 IEEE International Solid-State Circuits Conference (IEEE Cat. No.04CH37519)*, 2004, 318–530 Vol.1. doi: [10.1109/ISSCC.2004.1332722](https://doi.org/10.1109/ISSCC.2004.1332722).
- [9] S.-Y. Lee, M. Y. Su, M.-C. Liang, Y.-Y. Chen, C.-H. Hsieh, C.-M. Yang, H.-Y. Lai, J.-W. Lin, and Q. Fang, “A programmable implantable microstimulator soc with wireless telemetry: Application in closed-loop endocardial stimulation for cardiac pacemaker,” *IEEE Transactions on Biomedical Circuits and Systems*, vol. 5, no. 6, pp. 511–522, 2011. doi: [10.1109/TBCAS.2011.2177661](https://doi.org/10.1109/TBCAS.2011.2177661).
- [10] N. Li, Z. Yi, Y. Ma, F. Xie, Y. Huang, Y. Tian, X. Dong, Y. Liu, X. Shao, Y. Li, L. Jin, J. Liu, Z. Xu, B. Yang, and H. Zhang, “Direct powering a real cardiac pacemaker by natural energy of a heartbeat,” *ACS Nano*, vol. 13, no. 3, pp. 2822–2830, 2019. doi: [10.1021/acsnano.8b08567](https://doi.org/10.1021/acsnano.8b08567).
- [11] D. Jiang, B. Shi, H. OuYang, Y. Fan, and Z. Wang, “Emerging implantable energy harvesters and self-powered implantable medical electronics,” *ACS Nano*, vol. XXXX, May 2020. doi: [10.1021/acsnano.9b08268](https://doi.org/10.1021/acsnano.9b08268).
- [12] J. Dickson, “On-chip high-voltage generation in mnos integrated circuits using an improved voltage multiplier technique,” *IEEE Journal of Solid-State Circuits*, vol. 11, no. 3, pp. 374–378, 1976. doi: [10.1109/JSSC.1976.1050739](https://doi.org/10.1109/JSSC.1976.1050739).
- [13] H. Dadhich, V. Maurya, K. Verma, and S. Jaiswal, “Design and analysis of different type of charge pump using cmos technology,” in *2016 International Conference on Advances in Computing, Communications and Informatics (ICACCI)*, 2016, pp. 294–298. doi: [10.1109/ICACCI.2016.7732062](https://doi.org/10.1109/ICACCI.2016.7732062).
- [14] V. Mudeng, Y. T. Kusuma Priyanto, H. Wicaksono, V. A. Kusuma, and M. Muntaha, “Design of five stages cockcroft-walton with passive filter,” in *2019 6th International Conference on Electric Vehicular Technology (ICEVT)*, 2019, pp. 393–396. doi: [10.1109/ICEVT48285.2019.8993983](https://doi.org/10.1109/ICEVT48285.2019.8993983).
- [15] T. Langdon, “Very low power cockcroft-walton voltage multiplier for rf energy harvesting applications,” 2019.

- [16] M. Eid and E. Rodriguez-Villegas, “Analysis and design of cross-coupled charge pump for low power on chip applications,” *Microelectronics Journal*, vol. 66, pp. 9–17, Aug. 2017. DOI: [10.1016/j.mejo.2017.05.013](https://doi.org/10.1016/j.mejo.2017.05.013).
- [17] A. Ballo, A. Grasso, and G. Palumbo, “A review of charge pump topologies for the power management of iot nodes,” *Electronics*, vol. 8, Apr. 2019. DOI: [10.3390/electronics8050480](https://doi.org/10.3390/electronics8050480).
- [18] D. Chauhan and L. Gupta, “Design of current mirror and telescopic ota using 0.18 μm technology.”
- [19] F. Sandoval and E. Hernández-Bernal, “Ring cmos not-based oscillators: Analysis and design,” *Journal of applied research and technology*, vol. 6, pp. 54–64, Apr. 2008. DOI: [10.22201/icat.16656423.2008.6.01.524](https://doi.org/10.22201/icat.16656423.2008.6.01.524).
- [20] M. Kulkarni and V. Agrawal, “A tutorial on battery simulation-matching power source to electronic system,” Jan. 2010.
- [21] A. Rahmoun and H. Biechl, “Modelling of li-ion batteries using equivalent circuit diagrams,” *PRZEGLAD ELEKTROTECHNICZNY (Electr. Rev.)*, vol. 88, pp. 152–156, Jan. 2013.